HELSINGIN YLIOPISTO
HELSINGFORS UNIVERSITET
UNIVERSITY OF HELSINKI

Characterization of Human Pubertal Timing Gene *VGLL3* in Zebrafish Development

University of Helsinki

Faculty of Biological and Environmental Sciences

Department of Biosciences

Degree Programme in Molecular Biosciences

Master's thesis

Genetics

Spring 2017

Jana Pennonen

HELSINGIN YLIOPISTO

Tiedekunta - Fakultet - Faculty	Laitos - Institution - Department	
Bio- ja ympäristötieteellinen tiedekunta	Biotieteiden laitos	
Tekijä - Författare - Author		
Jana Pennonen		
Työn nimi - Arbetets titel		
Characterization of Human Pubertal Timing Gene VGLL3 in Zebrafish Development		
Oppiaine - Läroämne - Subject		
Perinnöllisyystiede		
Työn laji - Arbetets art – Level	Aika - Datum - Month and year	Sivumäärä - Sidoantal - Number of pages
Pro gradu -tutkielma	3.2017	55 s. + 2 liitettä

Tiivistelmä - Referat - Abstract

Murrosikä eli puberteetti on kehitysvaihe, jolloin yksilö kehittyy sukukypsäksi. Murrosiän ajoittuminen ihmisillä vaihtelee paljon sekä sukupuolen sisällä että sukupuolten ja populaatioiden välillä. Murrosiän ajoittuminen on monitekijäinen ominaisuus eli sekä perimä että ympäristötekijät vaikuttavat ajoittumiseen. Poikkeuksellisen varhainen murrosikä on liitetty erilaisiin aineenvaihduntasairauksiin kuten lihavuuteen ja II-tyypin diabetekseen sekä muihin sairauksiin kuten munasarja- ja kivessyöpään. Vaikka perinnöllisten tekijöiden arvioidaan selittävän n. 50-80% murrosiän ajoittumisen vaihtelusta, murrosiän geneettistä taustaa ei kuitenkaan tunneta kovin hyvin.

Genominlaajuisissa assosiaatiotutkimuksissa on hiljattain selvitetty murrosiän ajoittumiseen vaikuttavia geneettisiä lokuksia. Yksi näistä assosiaatioista oli geeni vestigial-like family member 3 (*VGLL3*). Tässä pro gradu -työssä keskityttiin selvittämään mekanismeja, joilla sukukypsyyden ajoittumiseen niin ihmisillä kuin lohella (*Salmo salar*) vaikuttava *VGLL3*-geeni toimii. Koska murrosiän kannalta tärkeimmät fyysiset rakenteet, mukaan lukien hypotalamus ja aivolisäke, muodostuvat jo alkionkehityksen aikana, ja nämä rakenteet ovat säilyneet evoluutiossa kaikilla selkärankaisilla, tavoitteena oli tutkia *vgll3*:n ilmentymistä ja mahdollista kehityksellistä roolia seeprakalan alkioilla.

Geenin ilmentymisen eli ekspression paikantamiseksi seeprakalan alkioissa on tässä työssä käytetty *in situ*-RNA -hybridisaatiotekniikkaa (ISH). Lisäksi geenin roolia on tutkittu yliekspressio- ja morfoliino-oligonukleotidi (MO)-knockdown -tekniikoilla, joiden avulla *vgll3*:n koodaaman proteiinin tuottoa on pyritty lisäämään ja hiljentämään muutaman päivän ikäisissä seeprakaloissa. MO:n ja synteettisen mRNA:n yhteisinjektiolla eli ns. rescue-kokeella on pyritty selvittämään johtuvatko havaitut fenotyypit nimenomaan *vgll3*:n expressiotason muutoksista.

ISH-kokeessa havaittiin *vgll3*:n ilmentyvän jo 0-1-päiväisillä alkioilla. Alle seitsemän tunnin ikäisillä alkioilla *vgll3*-mRNA:ta oli havaittavissa kaikissa soluissa, kun taas siitä vanhemmilla alkioilla *vgll3:n* ilmentyminen paikantui selkeästi rajattuihin kohtiin pään ja rungon alueella. Korkeat MO:n ja mRNA:n annokset geenieksprression muuttamiseksi varhaisissa alkioissa johtivat selkeisiin poikkeavuuksiin mukaan lukien lyhyeksi ja käyräksi jäänyt runkoakseli, sydänpussin ja ruskuaispussin turvotus sekä epämuodostunut pää ja silmät. Tutkimuksessa jäi kuitenkin avoimeksi, johtuivatko nämä tulokset yksinomaan *vgll3*:n ekspressiotason muutoksista.

Tutkimuksen tulosten perusteella voidaan olettaa, että *vgll3*:lla on mahdollisesti tärkeä rooli alkionkehityksessä. Tutkimuksessa ei kuitenkaan pystytty osoittamaan *vgll3:n* liittyvän selkärankaisten sukukypsyyden ajoittumiseen vaikuttamalla tunnettujen murrosikään liitettyjen rakenteiden, kuten hypotalamuksen, kehitykseen.

Avainsanat – Nyckelord - Keywords

murrosikä, puberteetti, vgll3, morfoliino, seeprakala, yliekspressio

Ohjaaja tai ohjaajat – Handledare – Supervisor or supervisors

LT, FT Elisabeth Widén; FM, tohtorikoulutettava Jaakko Leinonen

Säilytyspaikka - Förvaringsställe - Where deposited

Muita tietoja - Övriga uppgifter - Additional information


HELSINGIN YLIOPISTO

UNIVERSITY OF HELSINKI

Tiedekunta - Fakultet - Faculty	Laitos - Institution - Department	
Faculty of Biological and Environmental Sciences	Department of Biosciences	
Tekijä - Författare - Author		
Jana Pennonen		
Työn nimi - Arbetets titel		
Characterization of Human Pubertal Timing Gene VGLL3 in Zebrafish Development		
Oppiaine - Läroämne - Subject		
Genetics		
Työn laji - Arbetets art - Level	Aika - Datum - Month and year	Sivumäärä - Sidoantal - Number of pages
Master's Thesis	3.2017	55 p. + 2 appendices

Tiivistelmä - Referat - Abstract

Puberty is a process of physiological changes, through which an immature individual becomes sexually mature. In humans, timing of puberty is highly variable within and between sexes and populations. Timing of puberty represents a complex trait, which is controlled both genetically and environmentally. Precocious pubertal timing is associated with development of metabolic diseases later in life, such as obesity and diabetes, and other disorders as ovarian and testicular cancer. Despite the estimated high heritability (50-80%) of pubertal timing, its genetic background is still poorly understood.

Recently, the genome-wide association studies (GWASs) revealed many novel pubertal timing associated loci. Nevertheless, molecular mechanisms behind these associations remain elusive. This thesis focused on gene vestigial-like family member 3 (*VGLL3*), which is associated with pubertal timing in humans and maturation in Atlantic salmon (*Salmo salar*). Since the main physical structures, such as the hypothalamus and the pituitary gland, needed in reaching puberty are evolutionary conserved and start to develop in vertebrates during embryogenesis, the aim was to study the expression patterns and role of *vgll3* in zebrafish (*Danio rerio*) during this period.

In order to localize expression patterns of the *vgll3* gene in zebrafish embryos, a whole-mount *in situ* RNA hybridization (ISH) was performed. mRNA overexpression and morpholino oligonucleotide (MO) knockdown techniques were used to alter the *vgll3* gene expression levels in 0-5 dpf zebrafish. The combined injections of both mRNA and MO were performed to validate MO specificity.

The ISH experiment showed the expression patterns in 0-1 dpf embryos. The expression was ubiquitous up to 6 hours post fertilization becoming more localized to specific regions in the head and trunk of the embryos during the later stages. Altering *vgll3* expression with high concentrations of synthetic mRNA or MO lead to phenotypical abnormalities such as shortened and curved body axis, pericardial and yolk sack edemas, deformed heads and eyes. However, it remained unclear if these malformations appear only due to the alteration of *vgll3* expression levels.

The results suggest that *vgll3* may play an important role in the embryonic development. However, the study does not show that *vgll3* has impacts on the pubertal timing in vertebrates by affecting the development of the structures required for sexual maturation.

Avainsanat – Nyckelord - Keywords

puberty, timing, vestigial-like 3, vgll3, morpholino, zebrafish, knockdown, overexpression

Ohjaaja tai ohjaajat – Handledare – Supervisor or supervisors

MD, PhD Elisabeth Widén; MSc Jaakko Leinonen

Säilytyspaikka - Förvaringsställe - Where deposited

Muita tietoja - Övriga uppgifter - Additional information

Contents

LIST OF TERMS AND ABBREVIATIONS

Term/Abb.	Meaning
AAM	Age at menarche
Adipogenesis	A process, during which preadipocytes mature to the adipocytes
BMI	Body mass index
dpf	Days post fertilization
GnRH	Gonadotrophin-releasing hormone
Gonads	Reproductive glands
Gonadogenesis	A process, during which gonads develop
GWAS	Genome-wide association study
hpf	Hours post fertilization
HPG axis	Hypothalamic-pituitary-gonadal axis
KAL	Kallmann Syndrome Interval Gene
LIN28B	Lin-28 homolog B
MO	Morpholino oligonucleotide
Morphant	MO-treated organism
Myotomes	A group of muscles innervated by a single spinal nerve root
o/n	Overnight
PTU	Phenylthiourea
Somites	Divisions along head-to-tail axis in embryos
VGLL3	Vestigial-like family member 3
WT	wild type

1 Introduction

Puberty is an important milestone in every individual's life, during which the maturation of reproductive system occurs. A period of puberty represents rapid physical, mental, and emotional changes (Aksglaede *et al.* 2008). Sexual maturation via puberty is characteristic for vertebrates from fish to mammals (Chen & Ge 2013).

The period of reproductive cycle is initiated via puberty, and later regulated by hypothalamic-pituitary-gonadal axis (HPG axis), which already forms during the embryogenesis (Chevrier *et al.* 2011; Sisk & Foster 2004). The hypothalamic gonadotropin-releasing hormone (GnRH) neurons are crucial controllers of the HPG axis. Migration of hypothalamic GnRH neurons from olfactory placode to hypothalamus, which occurs during embryonic development, is a crucial milestone towards reproduction. Altered migration of GnRH neurons or misbalance within the HPG axis often lead to reduced or absent fertility later in life (Raivio *et al.* 2007; Rugarli *et al.* 1999; Sykiotis *et al.* 2010).

Many empirical studies have shown that the timing of puberty is a complex trait, with both genome and environment influencing the variation in timing. Heritability of the pubertal timing is estimated to be around 50-80% (Gajdos *et al.* 2010). Precocious timing of puberty is associated with higher risks of several diseases i.e. type II diabetes, cardiovascular disease, testicular and breast cancer in humans. Besides the significance of understanding the human development, these health risks make genetic studies of human pubertal timing important. The topic has been studied for many decades. Nevertheless, at this point the mechanisms behind the pubertal timing still remain poorly understood. (Golub *et al.* 2008; Hiatt *et al.* 2009; Lakshman *et al.* 2009; Loesch *et al.* 1995; Tanner *et al.* 1966; Widén *et al.* 2012.)

Recently, genome-wide association studies (GWASs) have revealed over 100 loci associated with pubertal timing (Perry *et al.* 2014). Variants in some of

these loci likely affect hormonal bioactivity, the development of the HPG axis, the timing of the pubertal growth spurt and energy homeostasis in humans. Importantly, several of these loci, e.g. *LIN28B*, and *VGLL3*, implicate evolutionarily conserved genes, which are expressed already during the fetal life (Barbaux *et al.* 2012; Faucheux *et al.* 2010; Perry *et al.* 2014).

This thesis examines the hypothesis that *VGLL3* may have some role in the formation of the HPG axis during the embryogenesis. With the use of several methods, I aimed to study the gene's expression patterns and impacts of the up- and downregulation of the *VGLL3* gene expression during the embryogenesis.

2 Aims

The first aim of this thesis is to study the temporal and spatial expression patterns of zebrafish *VGLL3* homolog *vgll3*. The localization of the gene expression, based on the whole-mount RNA *in situ* hybridization, may show whether the gene expression co-localizes with the olfactory placode, hypothalamic or pituitary regions, and whether the gene possibly interferes with the formation of these structures.

The second aim is to study the possible roles of *vgll3* in embryonic development by down- and upregulating its expression.

3 Background

3.1 Neuroendocrine regulation of sexual maturation and reproduction

3.1.1 HPG axis

Sexual reproduction in vertebrates is regulated by hypothalamic-pituitary-gonadal (HPG) axis including cooperation of hypothalamus, anterior pituitary, and gonads. The HPG axis probably emerged in ancestral agnathans, jawless fish representing the earliest vertebrates (Sower *et al.* 2009; Takezaki *et al.* 2003). Although vertebrate subphylum has remarkable phenotypic, habitat and behavioral diversity, sexual maturation and reproduction in this phylum is controlled by evolutionarily conserved system (Dubois *et al.* 2002; Sower *et al.* 2009).

The hypothalamus and pituitary gland form during the early embryogenesis. Prenatal activity of hypothalamus and anterior pituitary is critical for the emergence and expansion of male genitalia, and gamete development in humans (Chevrier *et al.* 2011; Kuiri-Hänninen *et al.* 2014). As pointed out above, although the HPG axis is evolutionarily conserved among vertebrates, in zebrafish only hypothalamus and pituitary gland form during embryonic development. The gonadogenesis starts after 8 days post fertilization (dpf), when juvenile fish are already fully developed and capable of feeding themselves (Okuthe *et al.* 2014).

In vertebrates, an increase in the activity of the HPG axis triggers puberty. With mechanisms that are currently not well understood, the central nervous system (CNS) starts to signal with the hypothalamus, the bridge between the nervous and endocrine systems. Specific neurons in the hypothalamus start to increasingly produce and release gonadotropin-releasing hormone (GnRH), a trophic neurohormone, which stimulates the anterior lobe of pituitary. Pituitary in response starts to produce two gonadotropins, follicle-stimulating hormone (FSH) and luteinizing hormone (LH). FSH's function is to initiate and stimulate maturation of gametogenesis in both sexes. LH stimulates endocrine cells of the gon-

ads to produce steroid sex hormones including androgens, estrogens and progesterone (Nelson & Bulun 2001; Silverthorn 2013; Vadakkadath Meethal & Atwood 2005). The units of the HPG axis control one another with their hormonal products in top-down and bottom-up manners (Figure 1).

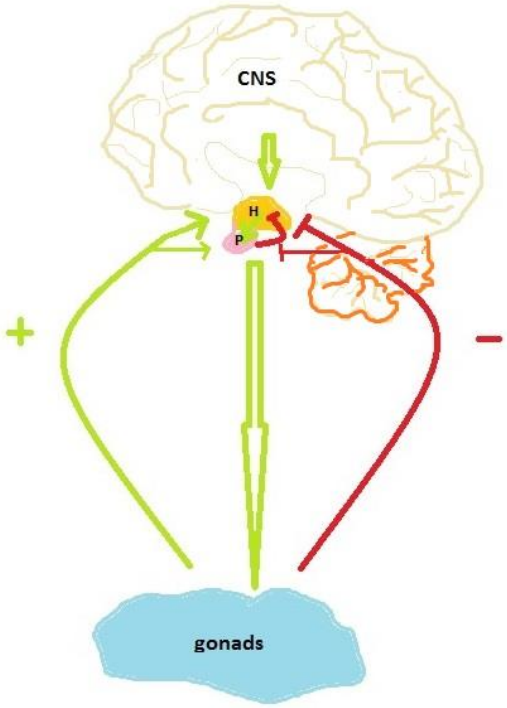

Figure 1. Green arrows in the middle demonstrate top-down control pathway, where GnRH from hypothalamus (H) affects secretion of LH and FSH by anterior pituitary (P). LH and FSH in turn stimulate gametogenesis and steroidogenesis in gonads. Green arrow on the left demonstrates long-loop positive feedback (hormone release stimulating, only estrogens) and red arrow on the right demonstrates long-loop negative feedback (hormone release inhibiting, estrogens and androgens) between gonads, anterior pituitary and hypothalamus. Red arrow between hypothalamus and anterior pituitary demonstrates short-loop negative feedback with LH and FSH affecting secretion of GnRH.

3.1.2 Development of the GnRH neurons and their connections to genetic factors causing HPG axis dysfunction

Increase in pulsatile secretion of hypothalamic GnRH is the initiating step in the pubertal activation of the HPG axis. Studies in comparative genomics have identified three paralogs of GnRH within vertebrates: GnRH1, GnRH2 and GnRH3 (primarily in modern teleosts) (White *et al.* 1998, Fernald & White

1999), of which zebrafish is known to have only GnRH2 and GnRH3 (Okubo & Nagahama 2008). The GnRH neurons first emerge in the olfactory placode and later migrate along vomeronasal nerves and via the cribriform plate, the boundary between the peripheral olfactory system and the forebrain, to the final destination in hypothalamus (Wierman *et al.* 2011). The GnRH neurons begin to migrate during the sixth week of gestation in human fetuses, whereas in zebrafish the migration starts around three dpf (Figure 2) (Abraham *et al.* 2009; Chevrier *et al.* 2011). Many factors influence the successful migration of GnRH neurons and not all mechanisms regulating the migration are fully understood (Wierman *et al.* 2011).

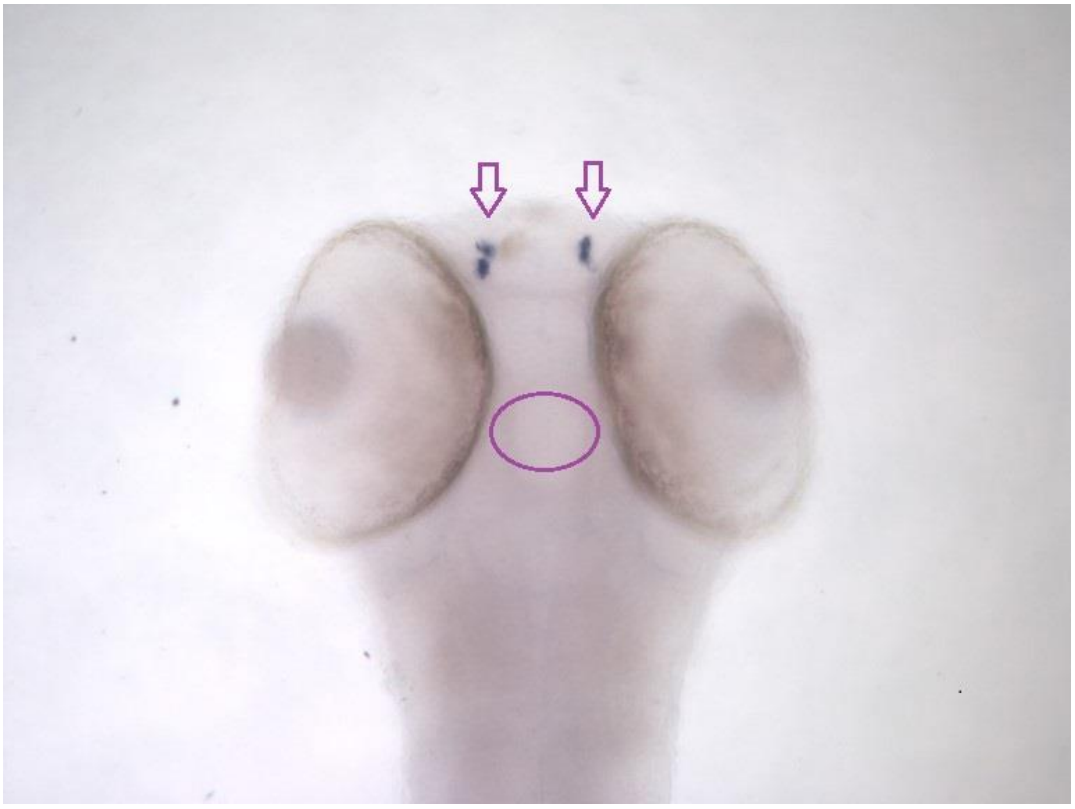

Figure 2. Whole-mount *in situ* hybridization of 3-days-old zebrafish larva. Expression of the *gnrh3* mRNA shown as dark purple signal. Arrows point regions of olfactory placodes. The approximate location of hypothalamus is framed in oval. Picture of the embryo was kindly provided by Jaakko Leinonen.

There are some conditions linked to delays or absence of puberty, caused by dysfunction within the HPG axis. The best characterized is isolated hypogonadotropic hypogonadism (IHH). These diseases are caused by events such as de-

fective specification or migration of GnRH neurons, or altered GnRH secretion (Sykiotis *et al.* 2010). Low levels of GnRH cause a collapse in the proper function of the HPG axis, which results in a delay or absence of puberty, and sterility in some cases. IHH can be categorized into two groups: normosmic IHH (patient has a normal sense of smell) and anosmic IHH or Kallmann syndrome. Anosmia is often the result of pathogenic mutations in crucial genes such as Kallmann Syndrome Interval Gene (*KAL*), which influences the migration of olfactory axons along with GnRH neurons out of the olfactory lobes. (Raivio *et al.* 2007; Rugarli *et al.* 1999; Sykiotis *et al.* 2010.)

Since the migration of the GnRH neurons is a key event required for further proper function of the HPG axis, exploring the possible relations of *VGLL3* to this process is one of this thesis' main aims.

3.2 Genetic background of pubertal timing

3.2.1 Genetic studies of puberty

The genetic background of many monogenic traits has been successfully studied by linkage analysis. The linkage analysis is based on searching for co-segregation of marker locus and locus of interest, and mainly used in studying familial monogenic diseases. For complex traits, such as pubertal timing in the general population, association studies to identify genetic loci affecting the trait have been more widely used. Association refers to a statistically significant correlation between a phenotype and marker alleles in a population. (Cantor *et al.* 2010; Perry *et al.* 2014; Pulst, S. M. 1999; Visscher *et al*. 2012.)

Several studies with population size ranging from few thousands to twenty thousand have shown that heritability of age at menarche (AAM), a marker for pubertal onset in females, is around 50-80% (Anderson *et al.* 2008; Gajdos *et al.* 2010; Towne *et al.* 2005). A more recent study (Morris *et al.* 2011) with a population size over 20 000, estimated that the heritability of AAM is around 57%. Linkage analyses have identified several monogenic disorders affecting

pubertal timing (Meitinger *et al*, 1990). However, as for many other complex traits, large-scale genome-wide association studies (GWAS) have successfully identified several loci affecting pubertal timing with small effect sizes (Visscher *et al*. 2012). Identification of pubertal loci through the experimental design of GWASs has been a subject of scientific interest for the last decade.

The region containing the *LIN28B* gene was the first significant AAM association (He *et al.* 2009). In another study (Elks *et al.* 2010), large data from 32 genome-wide association studies in 87,802 European women were handled with meta-analysis, revealing 30 new loci associated with pubertal timing. Currently, there are already over 100 genomic loci identified, although they together explain only ~2,71% of the genetic variability in AAM (Perry *et al.* 2014).

3.2.2 *VGLL3*, the focus of this thesis

Vestigial-like 3 (*VGLL3*) is one of the genes that have been associated with pubertal timing in the GWA studies. Two intergenic SNPs in this particular gene have been associated with pubertal timing related phenotypes. SNP rs7642134 has been associated with changes in AAM, weight, and BMI in European-American teen girls (Tu *et al.* 2014), and SNP rs7628864 with pubertal growth spurt and pubertal timing (Cousminer *et al.* 2013).

Remarkably, in two recent independent studies of maturational timing in Atlantic salmon (*Salmo salar*), two missense mutations in *vgll3* have been associated with early and late maturation in this species (Ayllon *et al.* 2015; Barson *et al.* 2015). Genetic variation in the *vgll3* locus explained 39,4% of variation in age at maturity in 57 salmon populations (Barson *et al.* 2015). Estimated effect of *vgll3* in Atlantic salmon is so high that it is suggested to be a major locus controlling the maturation age (Barson *et al.* 2015). Essentially, the human and salmon findings together suggest *VGLL3* having evolutionarily conserved functions in the regulation of pubertal timing in vertebrates.

At molecular level, *VGLL3,* from the vestigial-like gene family, encodes a transcriptional cofactor. The *vestigial* gene (*vg*), an ancestor of the *VGLL* gene fami-

ly, was first studied in *Drosophila*, where it has a key role in the development of specific flight muscles (Bernard 2003). The human *Vg* family includes *vestigial-like 1, 2, 3* and *4* (*VGLL1-4*) genes. Members of this gene family have similar function among vertebrates. All VGLLs contain at least one domain named tondu (TDU) motif, which interacts with transcriptional enhancer factor-1 (TEF) and guides it in cell differentiation processes (Chen *et al.* 2004a). Orthologous *Vgll2* and *Vgll4*, for example, regulate differentiation of specific muscle cell lines in mice, while expression of zebrafish *VGLL2* homolog has been linked to the formation of somites (Chen *et al.* 2004a and 2004b; Mann *et al.* 2007).

The human *VGLL3* has been localized to chromosome 3p12.3. Homolog of *VGLL3* has been studied as a potential tumor suppressor in ovarian epithelial tissues. The product of the gene has been also shown to act as an inhibitor of adipocyte differentiation in mouse 3T3-F442A and 3T3-L1 cell lines (Halperin *et al.* 2013). In these cells, *Vgll3* is downregulated during the terminal differentiation of adipocytes, and its overexpression or knockdown leads to changes in adipose tissue formation. *Vgll3* expression negatively correlates with the amount of body fat in mice. In mouse embryos, the expression of *Vgll3* has been observed in hindbrain area, myotomes and somites. In adult mice, the expression was present in skeletal muscle, heart, kidney, liver and brain. The gene expression was also detected in fetal mouse testis, suggesting that *Vgll3* has a role in testis development (Gambaro *et al.* 2013; Halperin *et al.* 2013; McDowell *et al.* 2012; Mielcarek *et al.* 2009). Similarly, in the frog *Xenopus laevis*, the expression of *vgll3* has been observed also in embryonic hindbrain area, and in brain, stomach and somites during embryogenesis. In adult frogs, expression of *vgll3* has been localized to stomach and heart tissues (Faucheux *et al.* 2010).

The molecular mechanisms linking *VGLL3* and the accumulation of adipose tissue remain poorly understood. It is also not clearly characterized, how and whether the expression of *Xenopus* and mouse *VGLL3* homologs influence the development of an embryo. Nor is it known what specific roles the gene has in adult mice and frog.

Because of the strong evidence that *VGLL3* has conserved functions among vertebrates, it is expected that similar expression patterns will be detected in developing zebrafish embryos as in mice or frog.

3.3 Fat accumulation and environmental influence on pubertal timing

In addition to genetic factors, environmental factors such as nutrition and overall health affect pubertal timing and growth (Tanner *et al.* 1966). Body growth, metabolism, and puberty initiation show strong correlation in many vertebrates, including mammals (Chen & Ge 2013). In rats (*Rattus norvegicus*), the onset of puberty correlates more with body size than with age (Kennedy & Mitra, 1963). In fish, puberty is also linked to the rate of accumulation of fat mass (Thorpe, 2004). In Atlantic salmon (*Salmo salar* L.), body size also correlates with reproductive success in females. Later maturing females that have increased size and body mass have higher fertility (Taranger *et al.* 2010). Similarly to salmon and humans, pubertal onset in zebrafish correlates with accumulation of fat and body size (Barson *et al.* 2015; Chen & Ge 2013).

3.4 Zebrafish as a model organism for this study

The zebrafish (*Danio rerio*) is a fresh water teleost and its original habitat is in Asian tropical streams. Zebrafish are small (4-5 cm in length), have clear sexual dimorphism, are easy to breed, feed and take care of. Zebrafish grow and develop fast: embryogenesis is completed in 50 hours post fertilization (hpf) and the fish reach reproductive age in 90-120 days (Figure 3). Developmental stages are clearly visible because of oviparity and late melanogenesis. Comparing with another popular vertebrate model, the mouse, zebrafish are cheaper to keep and feed, they need less space, they are faster to develop and produce much more offspring. There is around 70% of zebrafish genes that have orthologs in the human genome (Howe *et al.* 2013). These features explain why zebrafish have become a popular model organism, especially in studies of em-

bryonic development and modeling the function of human genes (Dooley & Zon 2000; Howe *et al.* 2013).

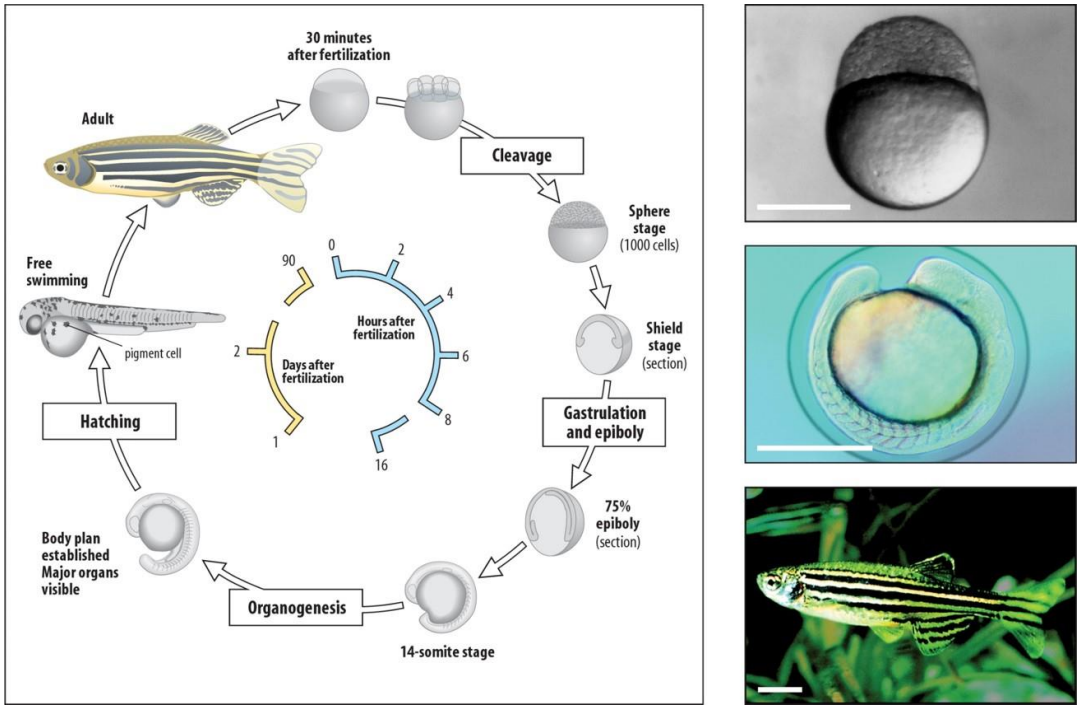

Figure 3. Life cycle of zebrafish. Organogenesis is complete after 24 hours post fertilization. Free-swimming stage starts between 2 and 3 days post fertilization (dpf). Complete maturation occurs around 90 dpf. Upper right image shows 1-cell stage embryo. Middle right photo shows around 1 dpf embryo with clear transparency. Lower right photo shows adult female. Figure was downloaded from: http://www.mun.ca/biology/desmid/brian/BIOL3530/DEVO_03/ch03f09.jpg

As typical for most vertebrates, the hypothalamus and pituitary gland in zebrafish start to develop during the early embryogenesis, and later the activation of the HPG axis initiates the puberty. Conserved mechanisms of hypothalamic GnRH play a critical role in the gonadal development, sexual maturation, and reproduction (Xu *et al.* 2011).

Studies have revealed at least four *vestigial-like* genes in zebrafish, and the *vgll3* has one-to-one homologous relation to the mammalian version (Figure 4). Comparison of the human VGLL3 protein and zebrafish vgll3 protein shows 40% sequence identity (Figure 5). With the recent study in Atlantic salmon revealing strong association between genetic variation in *vgll3* and age at matura-

tion (Barson *et al.* 2015), it is quite possible that *vgll3* could be a significant locus affecting age at maturity also in zebrafish.

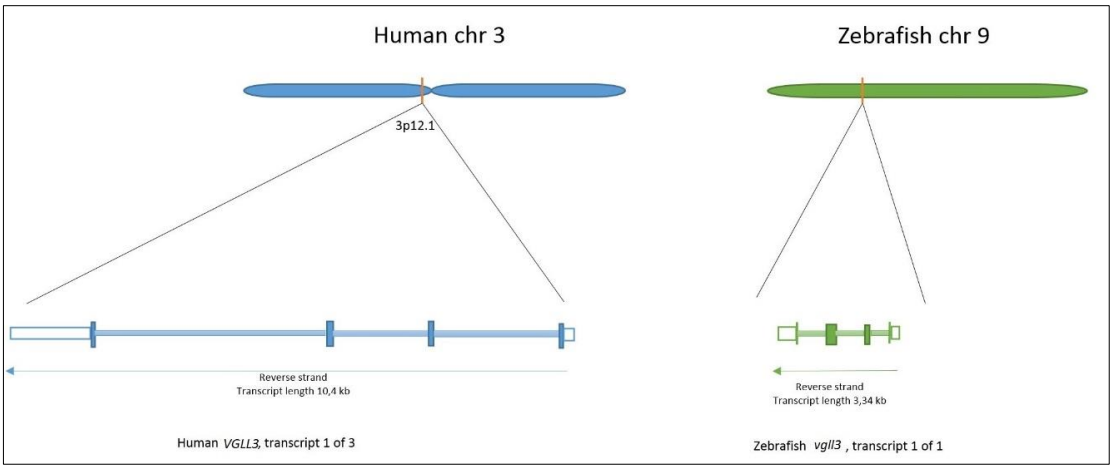

Figure 4. Figure showing position of *VGLL3* in human chromosome 3 and zebrafish chromosome 9. Both transcripts have 4 exons each. Unprocessed human *VGLL3* transcript shown in this figure is three times longer than zebrafish *vgll3* transcript. Figure is based on information from Ensembl (22.1.16)

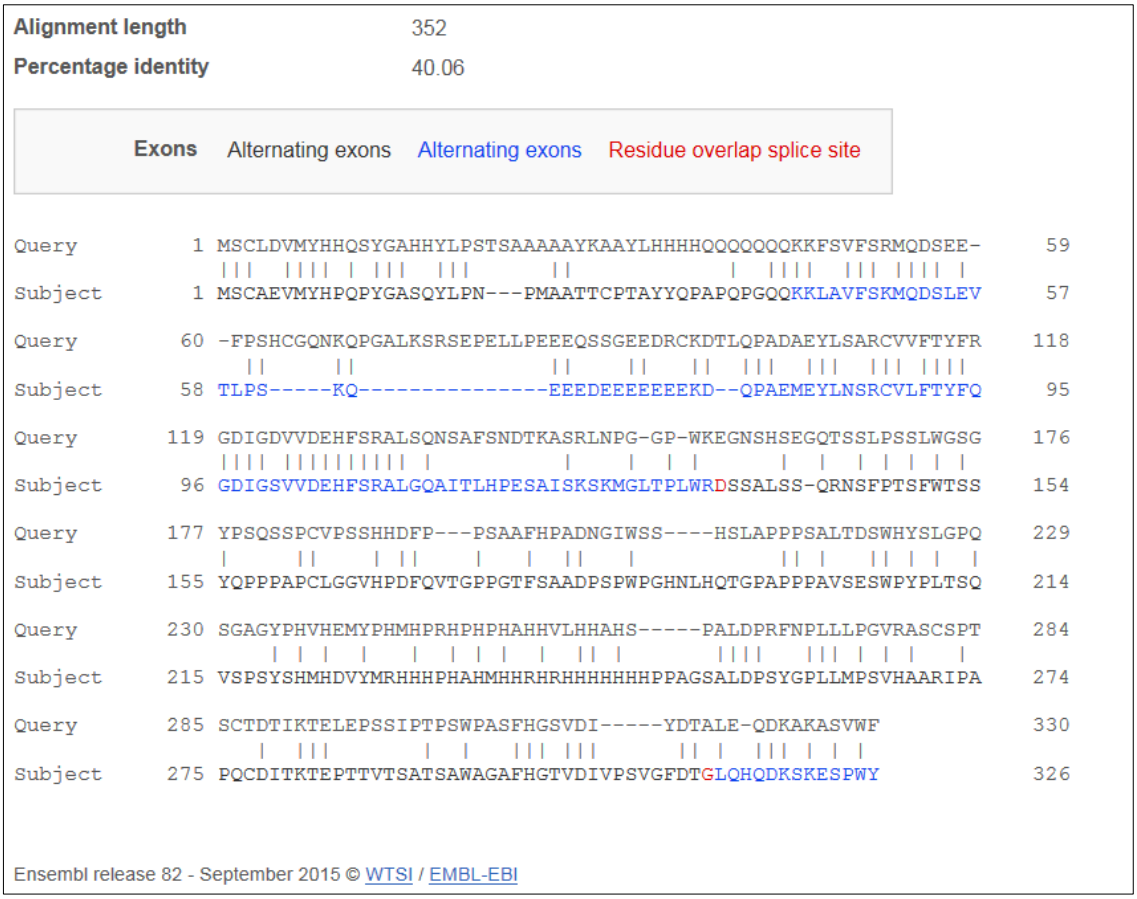

Figure 5. Sequence comparison of *Homo sapiens* and *Danio rerio* VGLL3 proteins showing ~40% identity in amino acid sequences (Ensembl).

3.5 In situ hybridization

In situ hybridization (ISH) is a technique that permits the detection of the expression of target genes at the DNA or mRNA level. The detection is achieved by a labeled DNA or RNA probe complementarity to the gene of interest. The ISH is performed by introducing the labeled radioactive or non-radioactive probe to the cell or tissue slides or, if small enough, to the whole organisms like zebrafish embryos (Hayes & Dutrillaux 2000; Thisse & Thisse 2008). The probes can be visualized either with autoradiography when using radioactive probes or via/with immunohistochemistry when non-radioactive probes are used (Jin & Lloyd 1997).

3.6 Knockdown and overexpression methods to study gene function in early zebrafish embryos

3.6.1 Morpholino as a knockdown tool

Morpholino oligonucleotides (MOs) are antisense nonionic nucleic acid analogs that have been used for 15 years in developmental biology for *in vivo* targeted inhibition of gene expression in embryos. Usage of MOs facilitates gene discovery through large-scale screening, characterization of gene function, and verifying mutant phenotypes. MOs have been used in several model organisms including *Xenopus* and chick (*Gallus gallus*). Easy delivery and high efficacy have made this knockdown technique widely used also in the zebrafish community (Bedell *et al.* 2011; Bill *et al.* 2009; Blum *et al.* 2015; Corey & Abrams 2001).

MOs are synthetic, relatively small (25 bp) and very stable imitations of DNA or RNA oligonucleotides, with two exceptions. MOs have a six-membered morpholine ring replacing (deoxy)ribose ring in the DNA/RNA molecules, and a non-ionic phosphorodiamidate backbone (Figure 6). MOs do not interact with RNase H, catalyzer of cleavage of RNA, because of morpholinos forming RNA-morpholino hybrids with their targets instead of natural RNA/DNA hybrids (Summerton 1999; Morcos 2007). The non-ionic properties of MOs prevent efficiently nonspecific interactions with other cell components e.g. proteins and allow MOs to easily penetrate through cell membrane (Bedell *et al.* 2011; Eisen & Smith 2008).

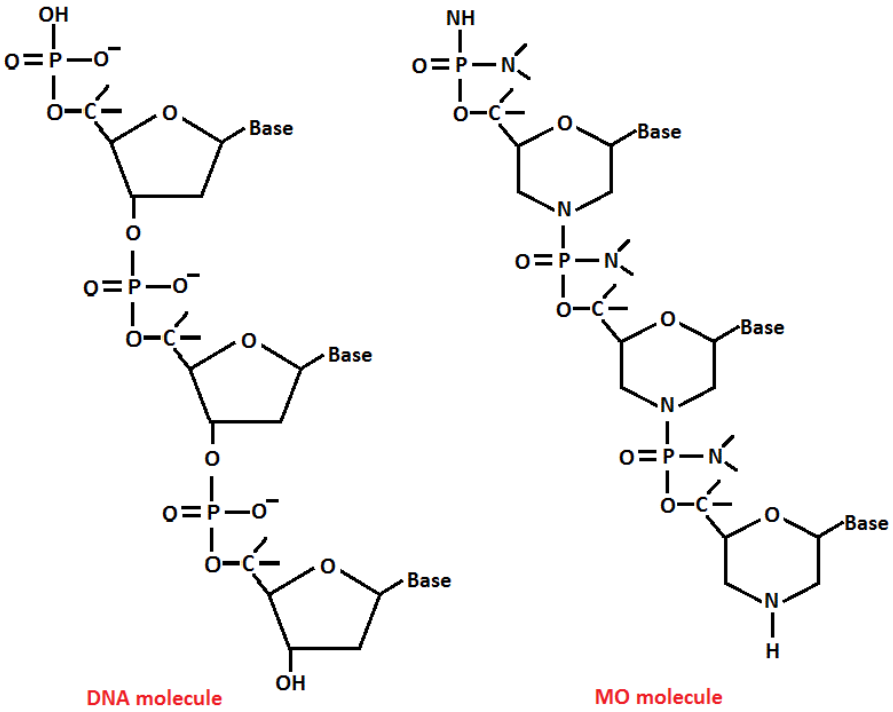

Figure 6. DNA molecule and MO molecule structures. The backbone of the DNA is ionic, while backbone of the MO is neutral because of an amino group replacing O^-.

Generally two types of morpholinos are used in research. Some morpholinos are designed to target the translational initiation site of an mRNA, overlapping an ATG codon coding for methionine and thus making mRNA invalid for translation. The second type includes morpholinos acting as splicing blockers through interrupting pre-mRNA splicing processes by targeting the splice donor site (Summerton 1999; Morcos 2007).

Despite their several advantages, morpholinos have been criticized for so-called off-target effects, which refer to their possible binding to unspecific transcripts or activation of cellular apoptosis pathways (Bedell *et al.* 2011; Bill *et al.* 2009; Blum *et al.* 2015; Corey & Abrams 2001). In zebrafish embryos, these off-target effects may cause p53-mediated programmed cell death and severe malformations. When target gene's function is unknown, it can be difficult to distinguish between gene-specific phenotype and off-target phenotype (Schulte-Merker & Stainier 2014). The use of standard control MOs, targeting an independent sequence, is usually recommended for cases when studying a gene

with unknown functions (Bedell *et al.* 2011; Eisen & Smith 2008). In early embryos (< 1 hpf), the tumor-suppressor gene p53 is usually highly expressed, thus presence of MO easily triggers the p53-mediated apoptosis processes (Cheng *et al.* 1997; Robu *et al.* 2007). This problem could be solved by inhibiting apoptosis with co-injections of p53-antisense MO. However, this method generates p53-absent genotype with unknown consequences, thus making knockdown resulting phenotypes less reliable (Schulte-Merker & Stainier 2014).

3.6.2 Synthetic mRNA as an overexpression tool

Synthetic mRNAs can be used as an overexpression tool for gene function studies. They have similar half-life and stability to a natural mRNA because of incorporated guanine cap on the 5′ end. The mRNA synthetization from the gene of interest is easy with commercial kits. Similarly to morpholinos, synthetic mRNA can be delivered into zebrafish embryos via microinjections (Warren *et al.* 2010; Yuan & Sun 2009).

3.6.3 Rescue method for MO phenotype validation

Co-injections of synthetic mRNA and MO for the gene of interest can be used to confirm the specificity of the MO. This strategy is called mRNA rescue, and is commonly used among zebrafish community (Bill *et al.* 2009). The idea of the rescue experiment is to prove that injected MO is interacting with the target mRNA, thus producing gene-specific phenotype. Synthetic mRNA restores the protein production, while the MO blocks the naturally occurring target mRNA. Rescue injections should contain both MO and mRNA in the correct concentrations and, when successful should produce wild type (WT)-like phenotypes. For successful validation it is important to avoid interactions between injected mRNA and MO, so injected mRNA should not contain a perfect match for MO binding site (Eisen & Smith 2008).

4 Materials and methods

4.1 Animals

The experiments were performed at the Zebrafish Unit in the University of Helsinki. All zebrafish procedures were carried out in accordance with the guidelines of the National Animal Experiment Board. All zebrafish used in the experiments were from Turku line, obtained from the Zebrafish Unit, and were maximum 5 days old. Adult zebrafish used for breeding were maintained at the zebrafish core-facility in the University of Helsinki, which has a site-specific license to house and breed fish.

4.2 Cloning *vgll3* for synthesis of RNA probes and mRNA

The extracted total RNA from 12 hpf embryos and 50 dpf zebrafish brain was used to clone *vgll3*. The RNA was converted into cDNA with SuperScript® VILO™ (Invitrogen, UK) cDNA Synthesis Kit (Table 1).

Table 1. Protocol for First-Strand cDNA synthesis

Component	Amount
5X VILO™ Reaction Mix	4 µl
10X SuperScript® Enzyme Mix	2 µl
RNA	8* or 11,5µl**
DEPC-treated water	up to 20 µl

* 12 hpf embryo RNA c=125 ng/µl, ** brain RNA c=90 ng/µl

1. Gently mix columns' contents and incubate at 25^{0}C for 10 minutes.
2. Incubate tubes at 42^{0}C for 2 hours.
3. Terminate the reaction at 85^{0}C at 5 minutes.

To amplify *vgll3* from prepared cDNA with PCR, primers were designed for the coding region of the zebrafish's *vgll3* gene based on sequence

(ENSDART00000099440) from Ensembl Genome Assembly GRCz10 database (https://www.ensembl.org/index.html) and obtained from Sigma-Aldrich® (Table 2).

Table 2. Primers for the *vgll3* cloning

Primer	Sequence (5'-3')	Tmº
VGLL3_Fw	CGCCTATAAGCCTCTG	54,1
VGLL3_R	GTGATGTATGTGGACCT	50,1

The primers were diluted before use for the working concentration of 5 µM. The components and the protocol used in *vgll3* PCR is shown below (Tables 3a and 3b). The PCR machine used in all amplifications was a G-Storm GS4 Multi Block Thermal Cycler (G-Storm Thermal Cyclers, Somerton, UK).

Table 3a. List of components for the PCR

Component	Amount
DreamTaq Green PCR Master Mix (Thermo Scientific)	10 µl
5 µM VGLL3_Fw primer	1 µl
5 µM VGLL3_R primer	1 µl
cDNA	2 µl
Nuclease-free water	6 µl
Total volume	20 µl

Table 3b. Protocol with 30 cycles for the PCR

Cycle step	Temperature	Time
Initial denaturation	95 ^{0}C	3 minutes
Denaturation	95 ^{0}C	30 seconds
Annealing	45 ^{0}C	20 seconds
Elongation	72 ^{0}C	3 minutes and 20 seconds
Final elongation	72 ^{0}C	10 minutes
Store	4^{0}C	∞

To separate the target DNA from other components of the PCR, I ran the PCR product on 1,5% agarose gel in Bio-Rad electrophoresis machine. To visualize DNA bands on the gel, the DNA fragments were stained with SYBR® safe DNA gel stain (ThermoFisher Scientific, MA, USA). After verifying the size of the target DNA the PCR product was extracted from the gel using a NucleoSpin® Gel and PCR Clean-up kit (Macherey-Nagel, PA, USA) following the manufacturer's protocol. The concentration of cleaned PCR product was determined with NanoDrop® ND-1000 Spectrophotometer (NanoDrop Technologies, Inc, DE, USA).

The extracted PCR fragment was inserted to pGEM®-T Easy vector, obtained from Promega (attachment 1). The pGEM®-T Easy contains the antibiotic resistance gene *amp*^{r}, and in case of successful transformation the bacteria colonies will grow on plates containing ampicillin and X-Gal culture medium.

Promega's quick protocol was used for ligation of the insert and vector, and transformation of recombinant vectors into bacteria. The post-ligational plasmid vectors were transformed to *Escherichia coli DH5α* strain, obtained from Professor Pertti Panula's lab (PP's lab, Neuroscience Center and Institute of Biomedicine, University of Helsinki). Bacteria were grown in falcon flasks containing liquid LB-medium in an incubator shaker for 20 h at 37^0C. Recombinant plasmids were extracted from the bacterial colonies using QIAprep® Spin Miniprep Kit (Qiagen) according to protocol for high-copy plasmid DNA. The integration of the *vgll3* insert was confirmed by performing PCR (Tables 4a and 4b) and sequencing the product at the Sequencing Unit of FIMM.

Table 4a. Components for the PCR used to confirm the presence of the insert and to produce template for sense and anti-sense mRNA-probe synthesis

Component	Amount
DreamTaq Green PCR Master Mix (Thermo Scientific)	10 µl
SP6 primer (PP's lab)	1 µl
T7 primer (PP's lab)	1 µl
Purified plasmid	1 µl

Nuclease-free water	7 µl
Total	20 µl

Table 4b. Protocol with 20 cycles for the PCR

Cycle step	Temp.	Time
Initial denaturation	95 ^{0}C	30 seconds
Denaturation	95 ^{0}C	10 seconds
Annealing	45 ^{0}C	20 seconds
Elongation	72 ^{0}C	30 seconds
Final elongation	72 ^{0}C	7 minutes
Store	4^{0}C	∞

4.3 Preparation of the RNA probes and labeling

In this thesis, the nonisotopic DIG-labeled RNA probe was chosen for the ISH experiment. The antisense and sense probes for *in situ* hybridization were synthesized using the *vgll3* PCR product amplified from the pGEM®-T Easy plasmids as a template, with DIG RNA Labeling Kits (SP6 for sense and T7 for antisense, Roche) according to the manufacturer's instructions. To localize *vgll3* expression in early developmental stages, ISH was performed to whole-mount zebrafish embryos according to a protocol introduced by Thisse & Thisse (2010). Altogether, zebrafish embryos from five different development stages (3, 6, 12, 24 and 48 hpf) were collected and stained. The 24 hpf and 48 hpf embryos were treated with 4% PTU for inhibition of the melanin synthesis. Every group contained 10 embryos for the antisense probe labeling, and 10 for the sense probe labeling as controls. The embryos were dechorionated and dehydrated according to Thisse & Thisse (2010).

4.4 Preparation of synthetic mRNA for injections

To prepare the synthetic mRNA for injections, the *vgll3* insert was further cloned into pMC plasmid vector (attachment 2). The pMC vector contains SP6 and T7 promoter sequences and poly(A)-tail sequence, enabling the synthesis of functional mRNA. To transfer the insert from pGEM®-T easy vector into pMC both vectors were cut using restriction enzyme EcoRI (NEB® CutSmart™). I used a Time-Saver™ (NEB) protocol with modified amount of components in the digestion of pMC and pGEM®-T easy vectors (Tables 5a and 5b).

Table 5a. Time-Saver™ components for digestion of the pMC easy vector

Component	Amount
Restriction enzyme	1,5 µl
plasmid DNA (c: 102 µg/ml)	15µl
10X NEBbuffer	7,5 µl
Nuclease-free water	51 µl
Total	75 µl

Table 5b. Time-Saver™ components for digestion of pGEM®-T easy vector

Component	Amount
Restriction enzyme	1 µl
plasmid DNA (c: 581,2 ng/µl)	2 µl
10X NEBbuffer	5 µl
Nuclease-free water	42 µl
Total	50 µl

After digestion pMC was purified with the MiniElute Reaction CleanUp kit (Qiagen), according to the manufacturer's protocol. To lower the risk of pMC vector's self-ligation, a dephosphorylation treatment with alkaline phosphatase was performed before the ligation with FastAp Thermosensitive Alkaline Phosphatase (ThermoFisher Scientific), according to the manufacturer's protocol.

For pGEM®-T easy containing the *vgll3* insert, the digested product was similarly purified with the MiniElute Reaction CleanUp kit and ran on an agarose gel to ensure that the *vgll3* insert was separated from the pGEM®-T easy properly. Thereafter, a ligation reaction including the cut and purified *vgll3* insert and pMC vector was performed according to the manufacturer's protocol with components shown below (Table 6).

Table 6. Components for the ligation

Component	Amount
Insert	1 µl
pMC plasmid	1 µl
Promega ligase	1 µl
2x ligase buffer	5 µl
Nuclease-free water	2 µl
Total	10 µl

pMC including the *vgll3* insert was subsequently transformed into *DH5α* bacteria and extracted from the bacterial colonies as in the chapter 4.1. Colony PCR (Tables 7a and 7b) was performed to detect the orientation of the insert in the purified plamids and verify insert's successful integration. The plasmids were sequenced by Sanger sequencing in the Sequencing Unit of FIMM. Subsequently, the plasmids were linearized with FastDigest ApaI restriction enzyme (ThermoFisher Scientific) according to manufacturer's protocol.

Table 7a. Components for the colony PCR

Component	Amount
Dream Taq Master Mix	10 µl
T7 OR SP6 primer (5 µM)	1 µl
VGLL3_R primer (5 µM)	1 µl
Nuclease-free water	8 µl
pipette tip of the colony	
Total	20 µl

Table 7b. Protocol with 30 cycles for the colony PCR

Cycle step	Temperature	Time
Initial denaturation	95 ^{0}C	5 minutes
Denaturation	95 ^{0}C	30 seconds
Annealing	50 ^{0}C	30 seconds
Elongation	72 ^{0}C	1 minute
Final elongation	72 ^{0}C	10 minutes
Store	4^{0}C	∞

After linearization, the product was purified with QIAgen MiniElute Reaction CleanUp kit and 2 µl of reaction was ran on agarose gel for verifying a successful linearization. Finally, capped mRNA was synthesised using the resulting linearized plasmid containing *vgll3* insert as a template, with mMESSAGE mMACHINE® T7 kit (ThermoFisher Scientific), according to the manufacturer's protocol. After synthetisation, RNA was stored in -80^{0}C until use.

4.5 mRNA microinjections

To overexpress *vgll3* mRNA transiently in zebrafish embryos, microinjections with synthetized mRNA were performed. The injections were made with an injector (WPI PV830 Pneumatic Pico Pump) and a micromanipulator (Narishige, Tokyo, Japan). Injection technique was similar with one described in Kardash's (2012) overview of methods used in zebrafish research. A dose of 4 nl (Table 8) was injected into the yolk of a 1-4-cell stage zebrafish embryos (Figure 7).

The embryos were injected with two different mRNA doses: 0,31 µl in mRNA-group 1 (*N*=30) and 0,65 µl in mRNA-group 2 (*N*=25) (Table 8). A WT group with uninjected fertilized eggs (*N*=30) served as a control. The development of embryos was monitored daily, and mortality and hatching rate recorded and abnormal phenotypes documented in all groups at 3 dpf.

Table 8. Microinjection mixture

	mRNA Group 1	mRNA Group 2
Injection volume	4 nl	4 nl
capped mRNA*	0,31 µl	0,65 µl
Phenol Red 0,5%	1 µl	1 µl
Water	3,7 µl	3,35 µl
Total	5 µl	5 µl
Working concentrations	0,125 ng mRNA/4 nl	0,255 ng RNA /4 nl

*mRNA c=498,6 ng/µl

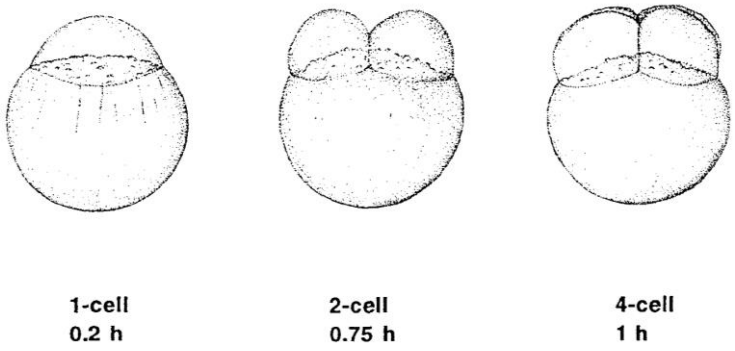

Figure 7. Illustrations of 1, 2, and 4-cell stage zebrafish embryos (Kimmel *et al.* 1995)

4.6 Morpholino oligonucleotide microinjections

Morpholino oligonucleotides (MO) were purchased from Gene Tools, LCC. Splice-blocking MO for *vgll3* was blasted against the zebrafish reference genome (build GRCz10) to ensure perfect match only to the target site. The obtained MO targeted exon 1-intron 1 splice donor site in pre-mRNA of *vgll3*. The negative control MO targeted a human beta-globin intron mutation that causes beta-thalassemia (Gene Tools). *p53* MO to control possible unspecific side effects was co-injected with *vgll3* blocking morpholinos. All MOs used in this thesis are listed below (Table 9).

Table 9. Morpholino oligo sequences complementarity to splice junction target of *vgll3* pre-mRNA, p53 mRNA and β-globin mRNA.

Name	Sequence (5'-3')
MO (zf_vgll3_ss1_block)	CCAACTTTACTCCCCTACCTGCTGC
p53 MO	GCGCCATTGCTTTGCAAGAATTG
control MO	CCTCTTACCTCAGTTACAATTTATA

Microinjections were carried out with an injector (WPI PV830 Pneumatic Pico Pump) and a micromanipulator (Narishige, Tokyo, Japan). A dose of 4 nl was injected into the yolk of a 1-4-cell stage zebrafish embryo. Knockdown experiment included four MO-injected groups (MO doses ranging from 1,5 to 6 ng), a control MO group and WT group as a negative control (Table 10). Groups 1,3, 4 and MO control contained 30 eggs in each and group 2 contained 25 eggs.

The development of embryos was monitored daily, and mortality and hatching rate recorded and abnormal phenotypes documented in all groups at 3 and 5 dpf.

Table 10. Microinjection mixture

	Group 1	**Group 2**	**Group 3**	**Group 4**	**MO control**
Injection volume	4 nl	4 nl	4 nl	4 nl	4 nl
Control oligo	-	-	-	-	1,2 µl
MO (1,0 mM)	0,3 µl	0,4 µl	0,6 µl	1,2 µl	-
p53 (1,0 mM)	0,6 µl	0,4 µl	0,6 µl	1,2 µl	-
Phenol Red 0,5%	1 µl	1 µl	1 µl	1 µl	1 µl
Water	3,7 µl	3,2 µl	2,8 µl	1,6 µl	2,8 µl
Total	5 µl	5 µl	5 µl	5 µl	5 µl
Working concentrations	1,5 ng MO /4 nl	2,0 ng MO /4 nl	3,0 ng MO/ 4 nl	6,0 ng MO/ 4 nl	6,0 ng St ctrl/ 4 nl

4.7 Rescue experiment

The rescue experiment was performed with two different MO/mRNA concentrations in each group (Table 11). There were 30 eggs in rescue-group 1 and 25 eggs in rescue-group 2 used. The splice-blocking MO and synthetic *vgll3* mRNA were injected into less than two hours post fertilized eggs. Control group included uninjected fertilized eggs.

Table 11. Rescue injections

	Group 1	**Group 2**
Injection volume	4 nl	4 nl
mRNA	0,31 µl	0,64 µl
MO (1,0 mM)	0,6 µl	0,4 µl
Phenol Red 0,5%	1 µl	1 µl
Water	3,1 µl	2,96 µl
Total	5 µl	5 µl
Working concentrations	3,0 ng MO + 0,125 ng mRNA	2,0 ng MO + 0,255 ng mRNA

4.8 Microscopy and Imaging

The morphology of the embryos and larvae from knockdown, overexpression and rescue experiments were examined under a Leica M125 inverted light microscope. Vgll3-labeled embryos were examined under Leica DM IRB inverted light microscope. Pictures of live embryos and larvae were taken with 2,5 megapixel microscope camera Leica MC120 HD, installed into the microscope and connected to a PC. Images of the embryos and the larvae were stored and edited with Leica Application Suite software and Photo Editor (By Chengdu Everimaging Science and Technology Co. Ltd).

5 Results

5.1 Temporal and spatial expression of *vgll3* in zebrafish embryos

The results from the *ISH* experiments showed that *vgll3* expression was detectable in all examined zebrafish embryos from 3 hpf to 24 hpf. At 3 hpf and 6 hpf *vgll3* was expressed ubiquitously in all cells (Figure 8). At 12 hpf strongest *vgll3* expression was detected in the hindbrain-midbrain area whereas at 24 hpf the expression became clearly localized in the developing hindbrain-midbrain area and the trunk (Figure 9). No expression patterns were visible in 48 hpf embryos stained with the vgll3 antisense probe (Figure 10). The embryos of the same ages in all five groups labeled with the sense probe showed no expression patterns, supporting the specificity of the observed hybridization signal.

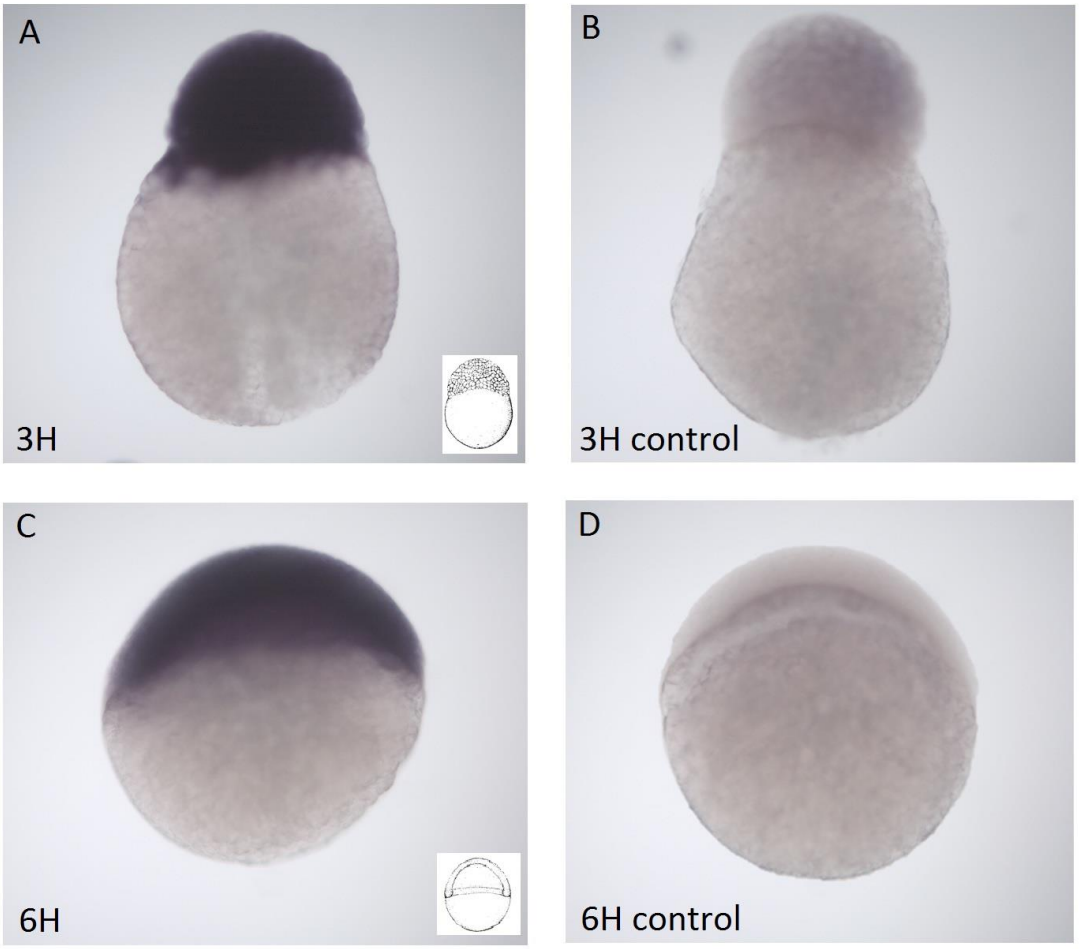

Figure 8. The figure shows 3 hpf embryos (A, B) and 6 hpf embryos (C, D). The animal pole is to the top. Ubiquitous expression of *vgll3* (dark purple stain) is observed at both developmental stages (A, C). The expression in 3 hpf (B) and 6 hpf (D) sense controls was not detected. Sketches shown in lower right corners (A, C) are adapted from Kimmel *et al*. (1995) publication.

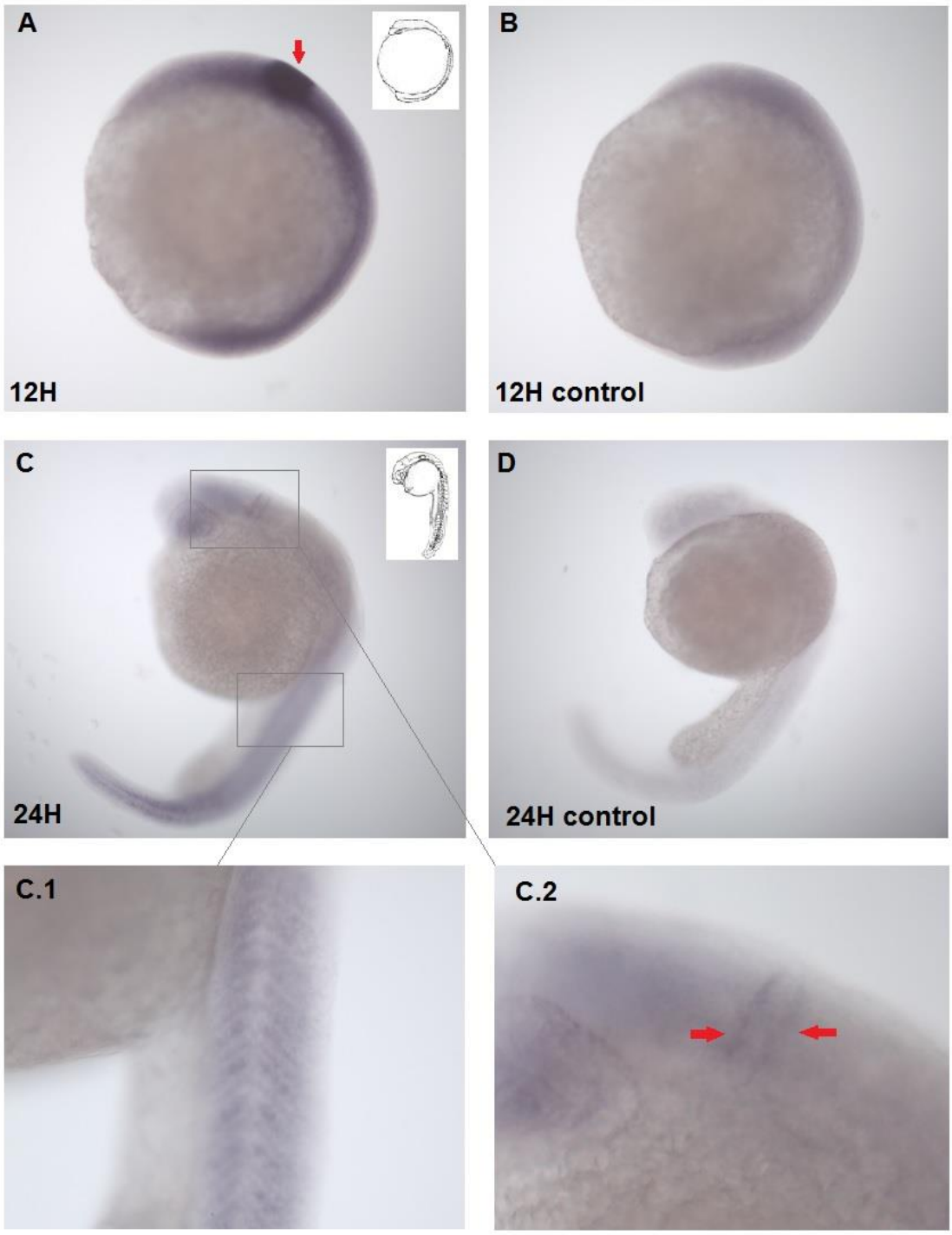

Figure 9. The figure shows 12 hpf embryos (A, B) and 24 hpf embryos (C, D). The anterior side of the embryos is to the top. In 12 hpf embryo, the expression (red arrow) is observed in the hindbrain rhombomere region (A). In 24 hpf embryo, *vgll3* expression is observed in the somites (C.1) and in the midbrain-hindbrain boundary (C.2, two red arrows). Expression in 12 hpf (B) and 24 hpf (D) sense controls was not detected. Sketches shown in the lower right corners of images A and C are adapted from Kimmel *et al*. (1995).

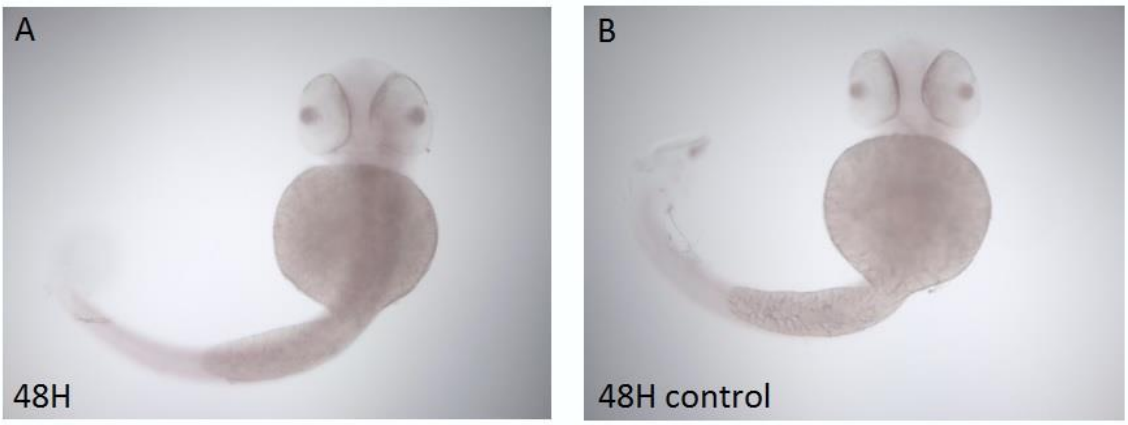

Figure 10. The figure shows whole-mounted 48 hpf embryos (A, B). The anterior end is to the top. The embryos show no detectable vgll3 expression during this stage.

5.2 Effects of knockdown of *vgll3* in zebrafish embryos

To assess the effects of knocking down *vgll3*, we injected 1- or 2-cell zebrafish embryos with combination of splice-blocking MO and p53 MO in four different concentrations. The degree of malformations and mortality in the injected groups clearly depended on the morpholino dose (Figure 11). Mortality of larvae observed at 5 dpf positively correlated with MO concentrations, ranging from 13% to 50%. Mortality of control MO larvae was 2.85 higher in comparison with the mortality of WT larvae (Figure 12). Showing a similar trend with mortality, the phenotypes of the MO injected fish varied according to MO dose (Figure 12). Hatching rate negatively correlated with concentrations of MO (Figure 13). On the contrary, despite the slightly increased mortality, larvae from the control MO injections had similar phenotypes compared to the WT.

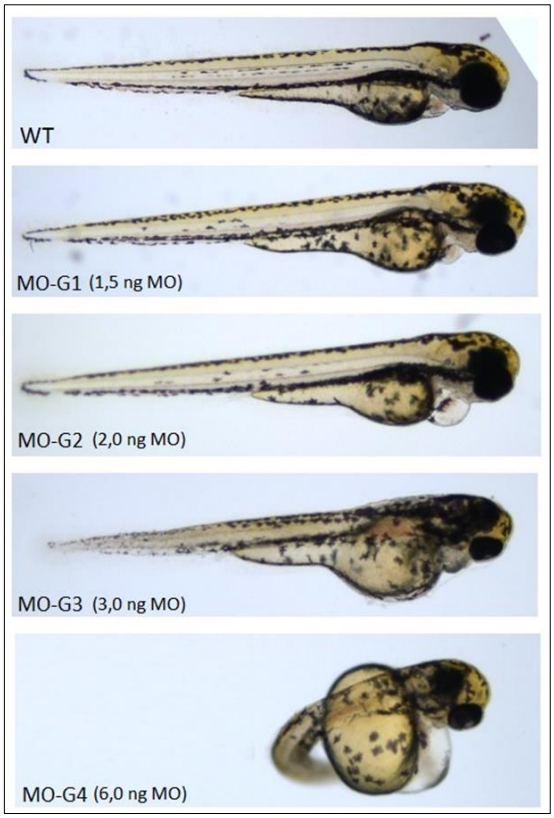

Figure 11. Overview of dose-dependent malformations in 3 dpf larvae. WT larva is shown on the top. Malformations become more severe when concentration of the MO increases from 1,5 ng to 6,0 ng. Common malformations detected were swollen head, smaller eyes, yolk sack edema, heart edema, and shortened and malformed body axis.

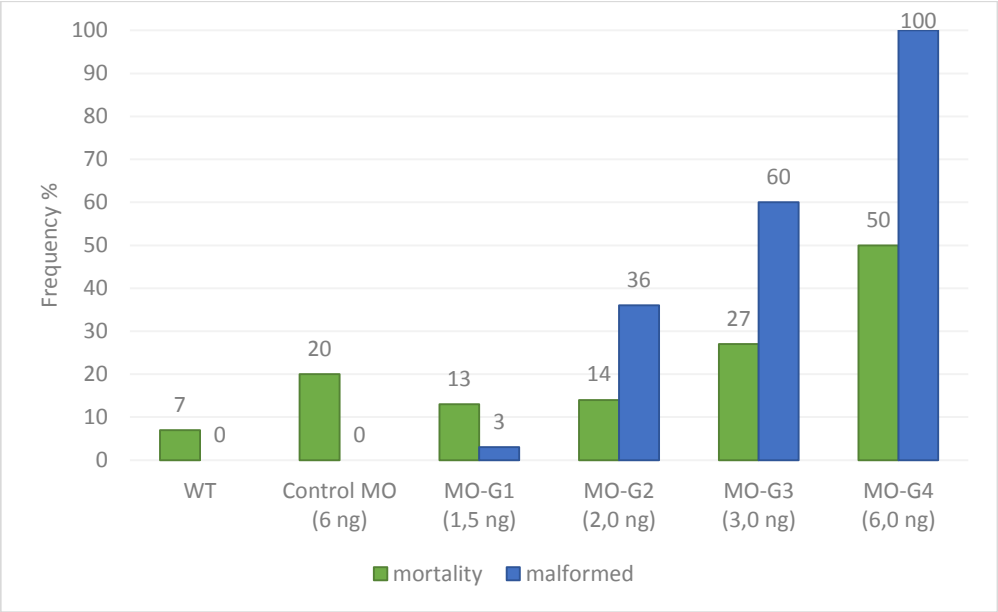

Figure 12. Mortality percentage (green) and percentage of fish with obvious malformations (blue) in all groups at 5 dpf. *N*=30 (g1, g3-4, control, WT), *N*=25 (g2)

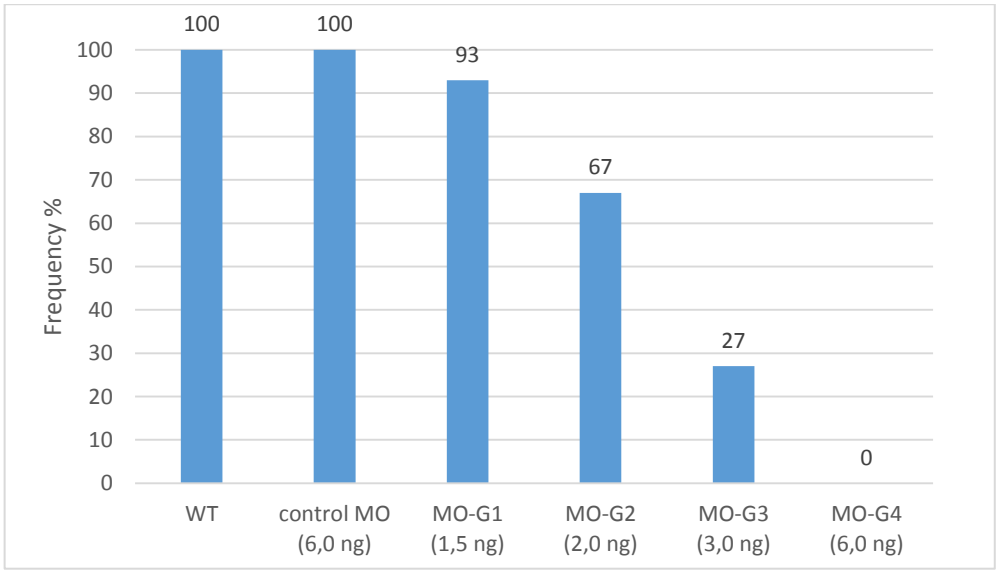

Figure 13. Hatched morphants and WT at 3 dpf, frequencies shown in percentage. Hatching rate remained the same after 3 dpf. *N*=30 (MO-G1, MO-G3-4, control, WT), *N*=25 (MO-G2)

The majority of larvae from MO-G1 group did not look phenotypically affected by the injections (Figure 14). About half of the larvae from MO-G2 had small pericardial edemas, but lacked any additional defects. The larvae from MO-G3 showed one or more of the following phenotypes: shortened and curved body axis, or both, swollen head, yolk sack edema, pericardial edema, abnormal localization of a heart, eye edema, eye malformations e.g. absence of anterior

chamber (Figure 15). The morphants from this group also appeared smaller, less pigmented and remained mainly passive to the response to external stimuli.

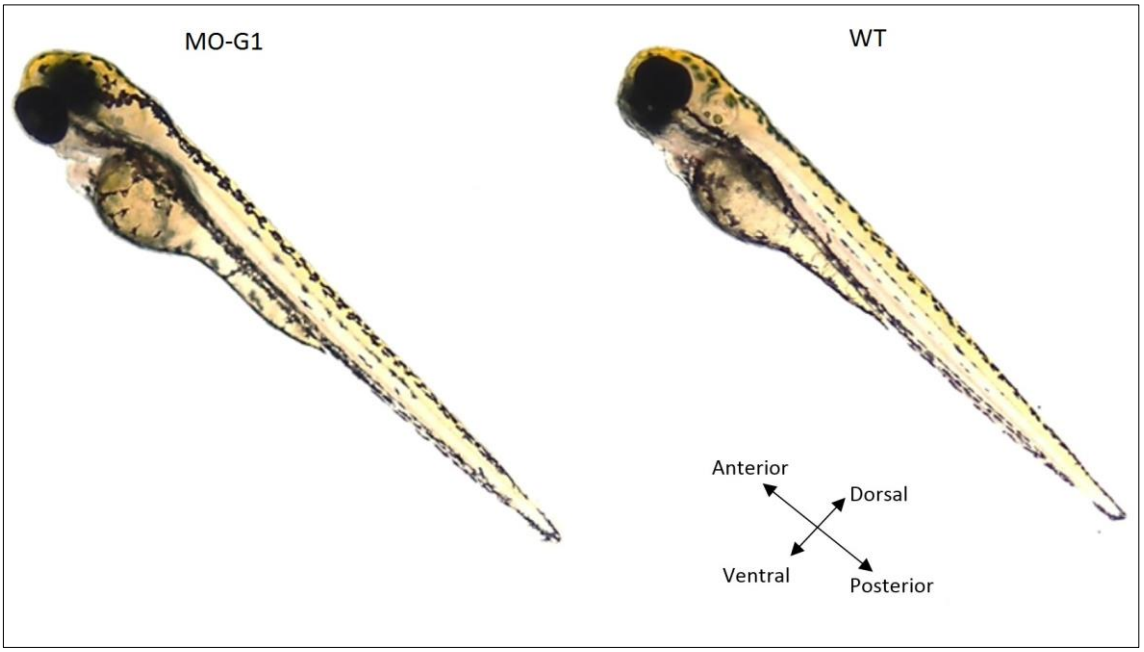

Figure 14. 3 dpf larva from MO-G1 on the left and 3 dpf WT larva on the right, with no clear phenotypical differences between the groups. *N*=30

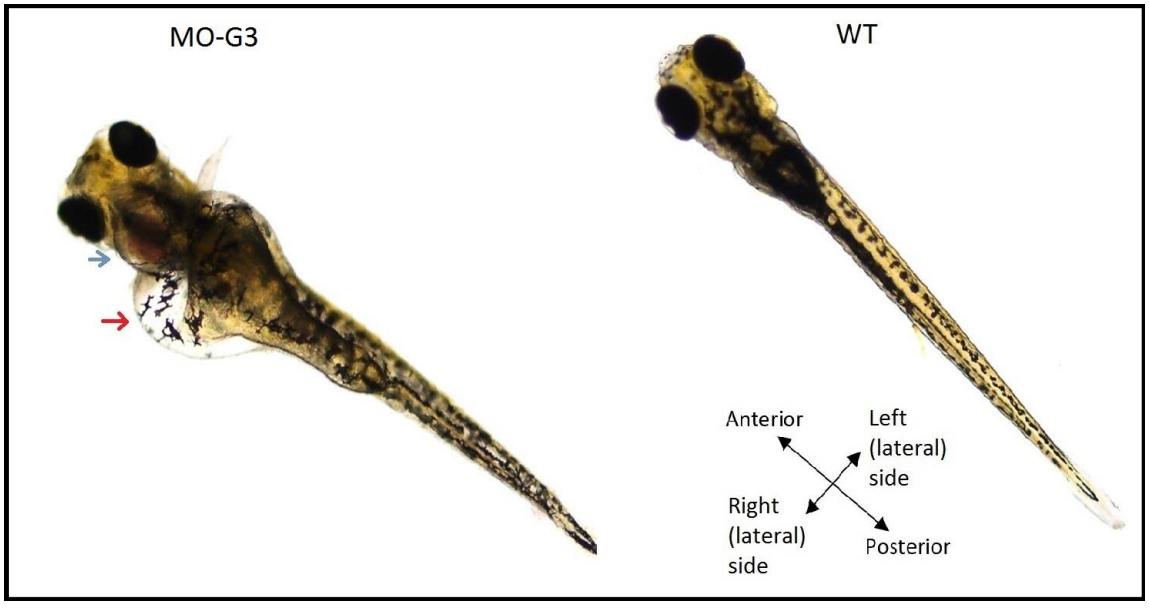

Figure 15. 5 dpf larva from MO-G3 on the left has a swollen head, yolk sack edema (red arrow), and pericardial edema (blue arrow). The features were typical for mal-

formed larvae from MO-G3 (MO *c*=3,0 ng/4nl). WT larva of same age is shown on the right. *N*=30

To validate the specificity of the phenotypic effects of the MOs, we performed rescue experiment using combined injections of *vgll3* mRNA and MO. The 1- or 2-cell embryos were injected with a combination of MO and mRNA. Embryos of R-G1 were injected with 3,0 ng MO and 0,125 ng mRNA, while embryos of R-G2 were injected with 2,0 ng MO and 0,255 ng mRNA. Unfortunately, we failed to validate the specificity of the MO induced phenotypes with this experiment. Both groups receiving a combined dose of MO and mRNA showed a high degree of mortality and abnormal phenotypes. On the contrary, the WT control fish were fully viable with no visible malformations. The mortality was slightly higher in R-G1 than in R-G2, but the frequencies of malformed phenotypes were similar in both R-groups (Figure 16), although R-G2 showed more severe phenotypes. The malformations observed in both groups included undeveloped heads, curved or kinked body axis, pericardial edemas and yolk sack edemas (Figures 17 and 18). The hatching rate in R-G2 was 5%, while in R-G1 it was 63% (Figure 19).

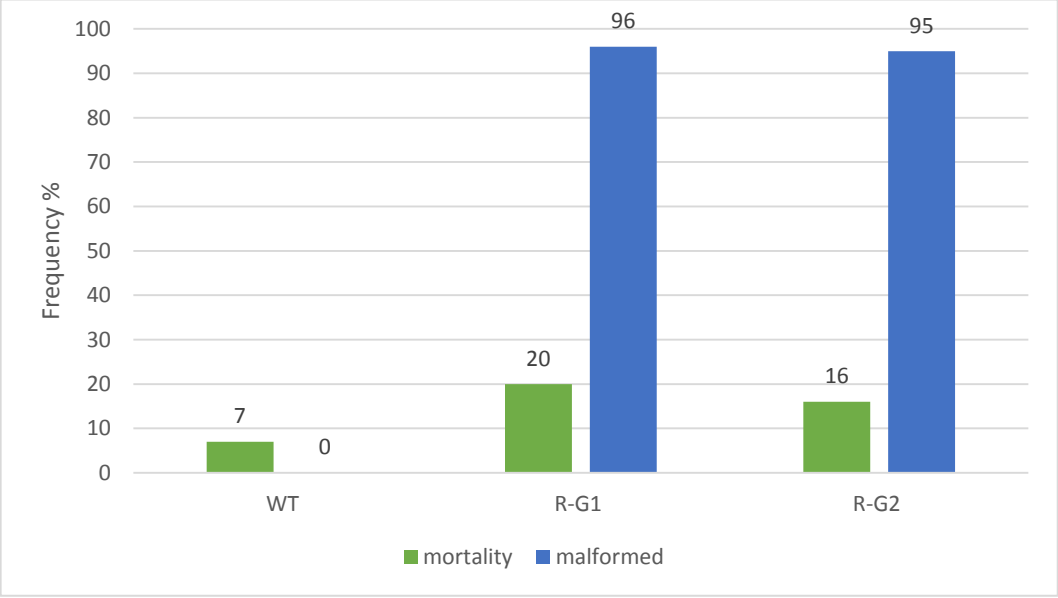

Figure 16. Mortality (green) and malformed phenotype (blue) frequencies in R-G1-2 and WT at 4 dpf. N=30 (R-G1, WT), N=25 (R-G2)

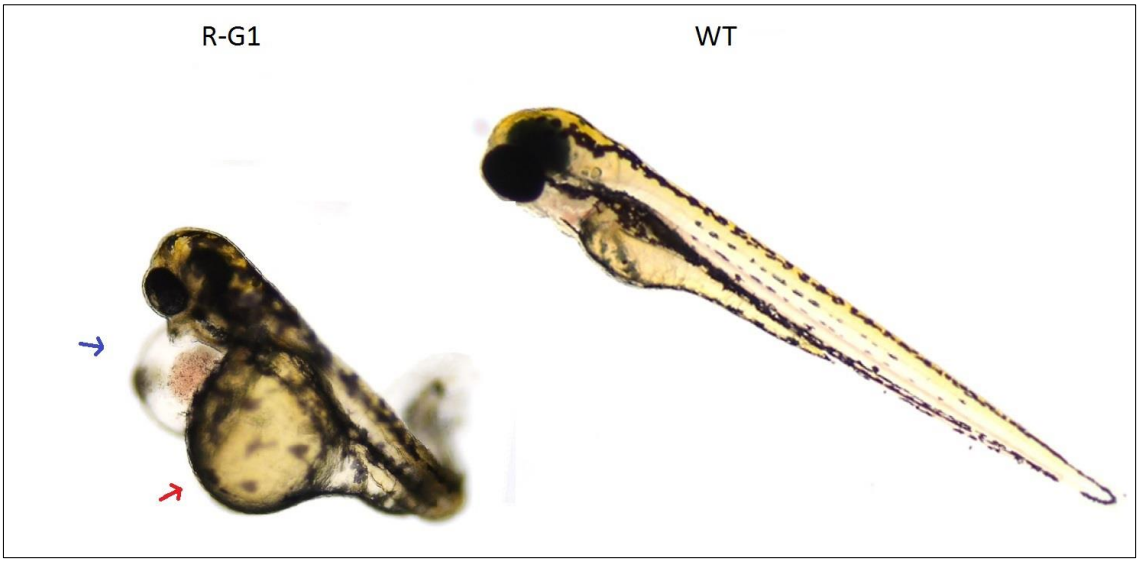

Figure 17. An image of a malformed larva at 3 dpf from R-G1 compared to WT of same age. Malformed larva has a small head, a pericardial edema (blue arrow), yolk sack edema (red arrow) and kinked body axis.

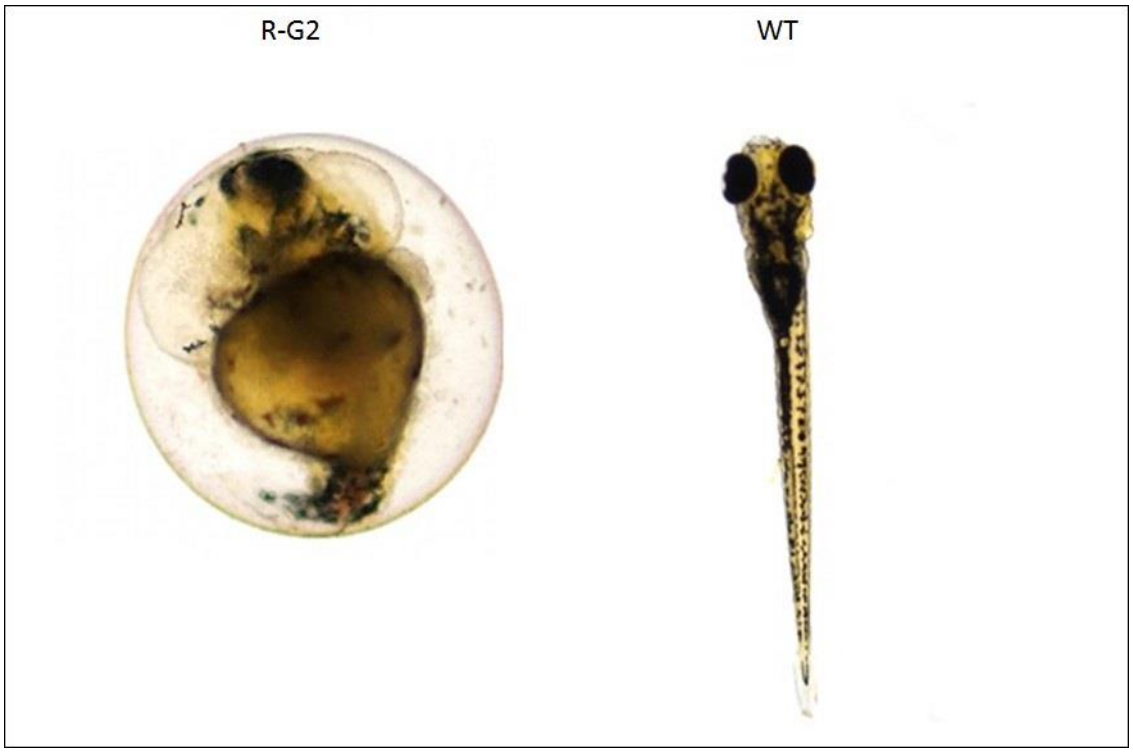

Figure 18. Unhatched, significantly malformed 4 dpf larva from R-G2 shown on the left. The larvae present significant yolk sack and pericardial edemas, undeveloped head and body axis. The WT larva of same age is shown on the right.

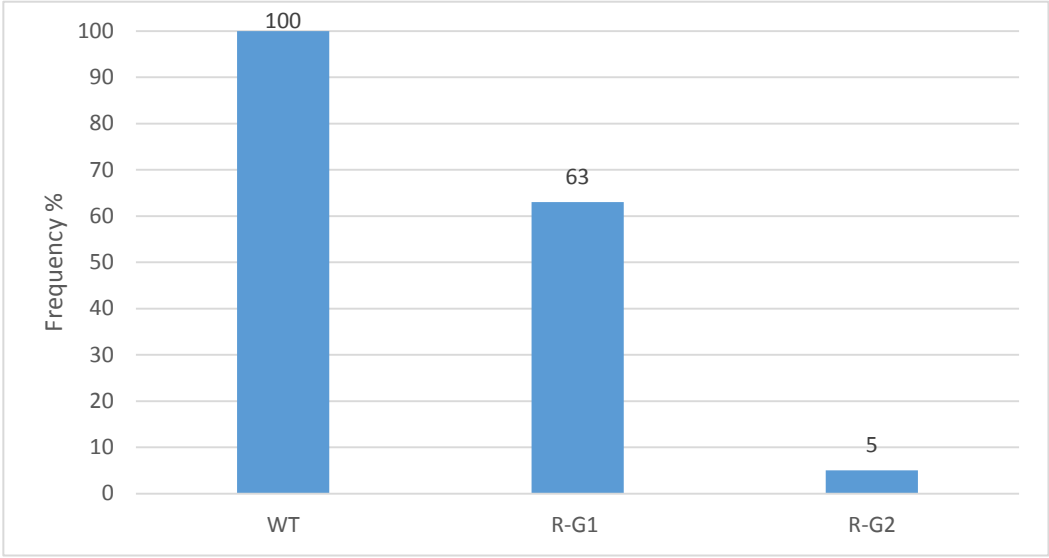

Figure 19. Frequency of hatching observed in the R-G1, R-G2 and WT groups from the rescue experiment.

5.3 Effects of overexpressing *vgll3* in zebrafish embryos

To assess the effects of *vgll3* overexpression in zebrafish embryos, we performed synthetic mRNA injections into zebrafish eggs. Similarly to the MO injected embryos, *vgll3* mRNA injected fish showed a range of abnormalities with the mRNA injections clearly affecting the development of the embryos. Unexpectedly, both phenotypic abnormalities and mortality in 3 dpf larvae correlated negatively with the mRNA concentrations (Figure 20). mRNA-G1 injected with 0,125 ng mRNA contained a high amount of significantly malformed larvae including fish with strongly shortened and curved body axis, pericardial edema, yolk sack edema, and swollen head (Figure 21). Larvae from mRNA-G2 injected with 0,255 ng mRNA had similar, but milder malformations in slightly over the half of the cases (Figure 22). Hatching frequency remained similar in all groups (Figure 23).

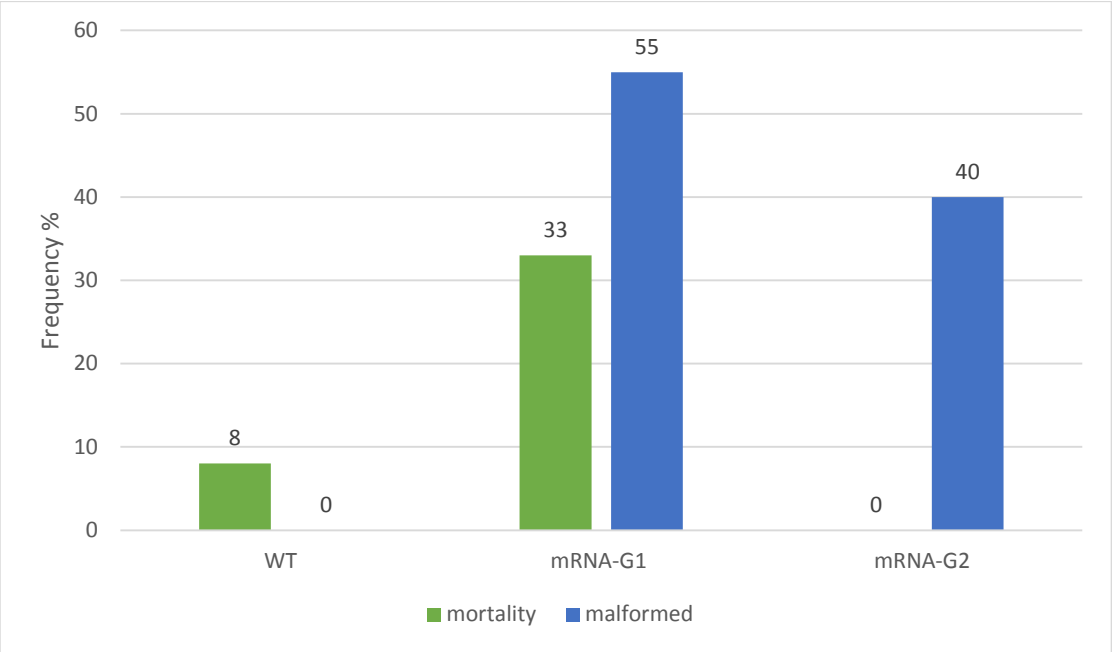

Figure 20. Mortality (green) and malformation (blue) frequencies in mRNA-G1, mRNA-G2 and WT on 3 dpf. *N* =30 (mRNA-G1 and WT), *N* =25 (mRNA-G2)

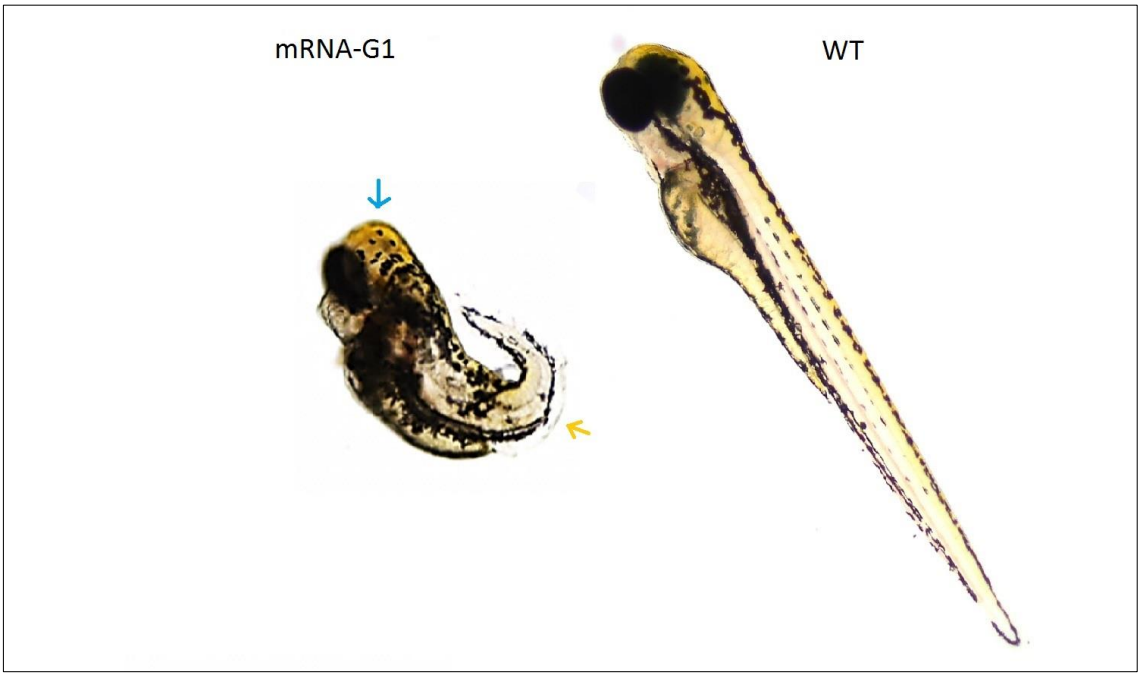

Figure 21. An example of a 3 dpf larva with malformations from the mRNA-group 1 on the left. The larva has swollen and undeveloped head (blue arrow) and clearly malformed body axis (orange arrow). WT larva of the same age is shown on the right.

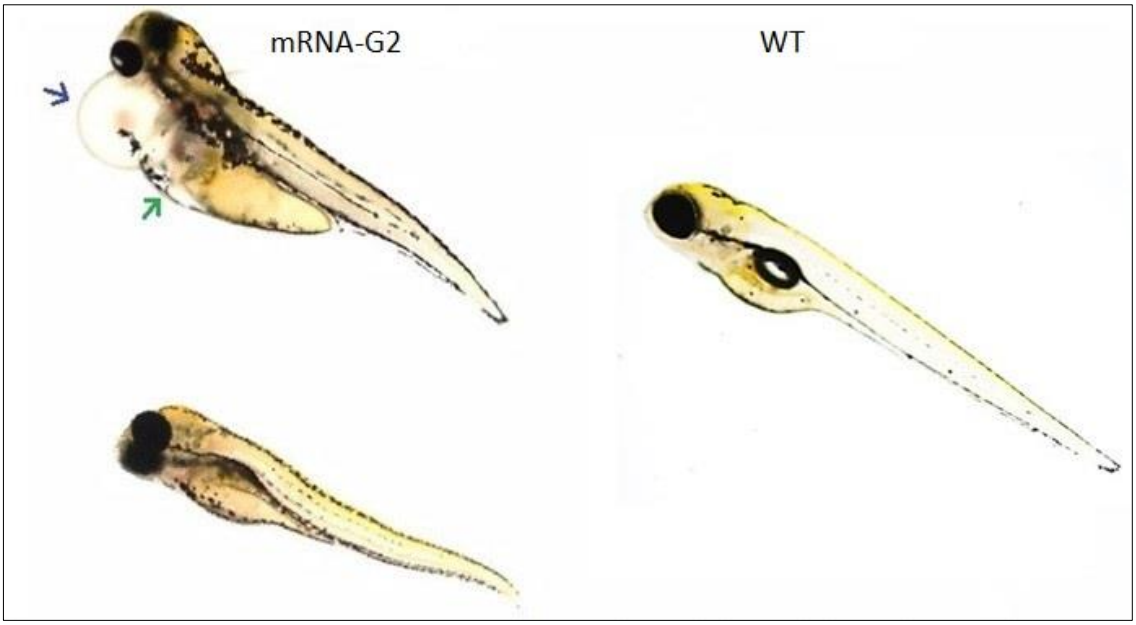

Figure 22. Two 4 dpf larvae with typical phenotypes from the mRNA-group 2 on the left. The larva in the upper left corner shows a dramatic phenotype with pericardial edema (blue arrow), yolk sack edema (green arrow), curved body axis and swollen head. The larva in the lower left corner shows phenotype with milder malformations. WT larva of the same age is shown on the right.

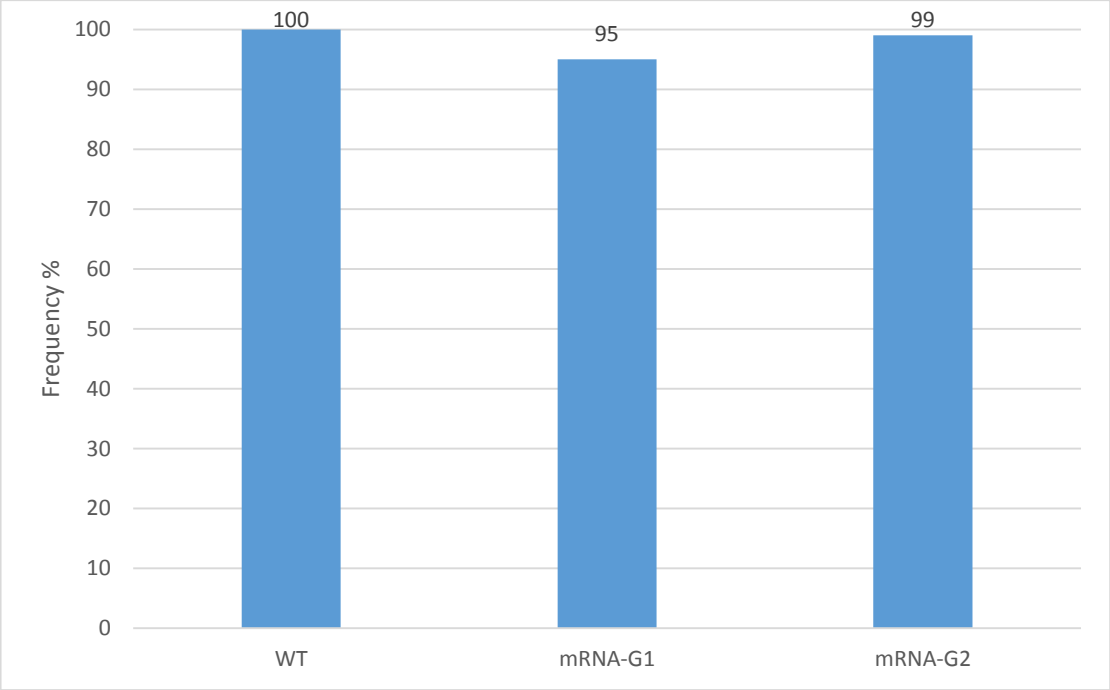

Figure 23. Hatching rate of mRNA-G1 and mRNA-G2 embryos recorded at 4 dpf. *N*=30 (group 1, WT), *N*=25 (group 2)

6 Discussion

VGLL3 is a transcriptional cofactor that has been associated with pubertal timing in humans and age at maturity in Atlantic salmon (Barson *et al.* 2015; Cousminer *et al.* 2013). However, molecular mechanisms of the gene behind sexual maturation in humans and fish remain unknown. This thesis was designed to explore two questions: 1) is the *VGLL3* homolog expressed during the development of zebrafish embryos and is the expression such that it can be linked to the formation of the HPG axis during the embryogenesis; and 2) what is the impact of up- and downregulation of *vgll3* expression during zebrafish embryonic development.

6.1 Expression of *vgll3* in WT embryos

The *in situ* hybridization experiment for zebrafish embryos repeated the previously reported embryonic expression patterns of *vgll3* in other model organisms (Gambaro *et al.* 2013; Faucheux *et al.* 2010; Halperin *et al.* 2013; McDowell *et al.* 2012; Mielcarek *et al.* 2009). The result strengthens the suggestion that the gene contributes to early vertebrate development in an evolutionarily conserved manner. However, the results from this study do not directly link *vgll3* to the development of the HPG-axis at least during the embryogenesis, and thus the gene's link to puberty remains elusive. However, for example in this study it was not possible to study the relation of the *vgll3* expression to the formation and development of gonads, due to gonadogenesis starting only around 8 dpf in zebrafish (Okuthe *et al.* 2014).

Although the study missed the link to puberty, the results from the *in situ* experiments provided several interesting results. The expression of *vgll3* was detected in four age groups out of five. The strongest signal was present in embryos at 3 hpf (512-cell) and 6 hpf (germ ring). At 3 hpf the embryo is entering a mid-

blastula period, during which the embryonic cells form a blastomeric sphere. The 6 hpf embryo is in the middle of the gastrula period, when the cells organize into three germ layers known as mesoderm, ectoderm and endoderm (Kimmel *et al.* 1995). Potentially, as a transcription cofactor, the role of *vgll3* during early embryogenesis could be similar to a role of any other transcription cofactor within regulatory networks, which regulate the cleavage and determinate the cell fate during segregation of the three germ layers (Khan *et al.* 2012; Peter & Davidson, 2010; Spitz & Furlong, 2012).

At 12 hpf (3-somite stage), a strong signal was observed in the future hindbrain region. At this stage, embryo undergoes segmentation process along the anterior-posterior axis, which includes generation of seven segments of hindbrain called rhombomeres (Kimmel *et al.* 1995). As described previously (Kimmel *et al.* 1995; Schilling *et al.* 2001), the rhombomeres are not morphologically divided (rhombomere boundaries are not developed) prior 18 hpf, thus at 3-somite stage it is not possible to link the observed expression pattern with a particular rhombomere.

At 24 hpf (prim-5 stage), I detected expression of *vgll3* in the midbrain-hindbrain boundary region, and in the trunk (somites) (section 5.1. Figure 9C). At this stage, the primordium of the cerebellum (anterior part of rhombomere1) and midbrain-hindrain boundary develop. Also, all 30 somites of the trunk are formed (Stickney *et al*.). This suggests that *vgll3* may play a role in the development of these regions of the embryo. Interestingly, the mouse and *Xenopus vgll3* homologs are also expressed in the hindbrain and somites at similar stages of embryonic development. This supports conserved mechanisms of *vgll3* among vertebrates (Faucheux *et al.* 2010; Mielcarek *et al.* 2009).

At 48 hpf (right before long-pec), the ISH experiment failed to show any expression of *vgll3*. The result suggests that either the gene is only weakly expressed during this stage, or there was a problem with the penetration of the probe into the embryos. If the gene truly is weakly expressed, a logical conclusion would be that *vgll3* lacks any functions in this development stage. For example, the absence of the gene expression could be partly explained by the fact that the

hindbrain and the somites have completed their formation prior 48 hpf (Kimmel *et al.* 1995; Stickney *et al.* 2000).

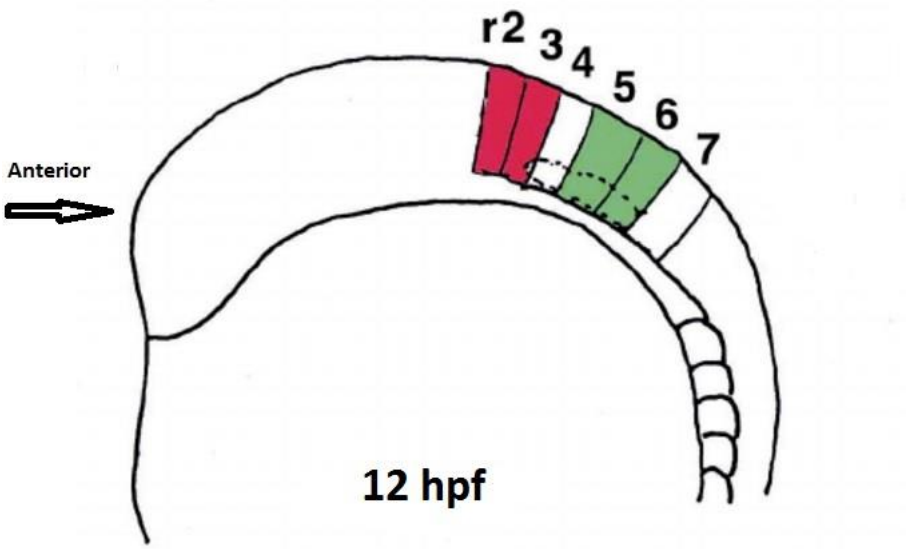

Figure 24. 12 hpf zebrafish embryo. Developing rhombomeres (without boundaries) are numbered from r2 to r7. The rhombomere division is presumptive. The figure is adapted from Schilling *et al*. (2001) paper.

Although in this thesis we did not try to characterize the molecular function of the *vgll3*, potentially, the function of *vgll3* could be similar or related to the function *vgll2*, showing a high degree of sequence homology. In mice*, Vgll2* is an important cofactor, which guides TEF-1 transcription factor during differentiation of specific muscle classes (Chen *et al.* 2004b; Mielcarek *et al.* 2009). Based on the observed expression patterns, it is possible, that in zebrafish *vgll3* exerts a similar guiding role for other transcription factors that participate in the formation of the hindbrain and the somites, or both.

6.2 Knockdown and overexpression of *vgll3*

In the knockdown experiment, I observed the expected concentration-dependent phenotypes in almost all MO-groups. However, I did not detect any

phenotypical effects of injections in the group with the lowest dose of MO (MO-G1, 1.5 ng). Observed absence of visible malformations in this group could be due to several reasons: First, the specific malformations occurred only in internal structures of embryos, thus they were not detectable with the optics used in this work. Second, the dose was not high enough to cause malformations or, finally, the gene could simply not have any important functions in the developing embryos. The reason can be also a combination of all. In the case of too small dose of MO, it is possible that *vgll3* codes for a protein with a long half-life or/and an efficient function with only small amount of gene product required. Therefore, the dose of 1.5 ng was not enough for proper gene knockdown. It is also possible that due to the small dose of MO the embryos were capable of producing more *vgll3* product for compensating the lost product amount.

Morphants of MO-groups 2,3 and 4 showed concentration-dependence in all observed phenotypes. Yet, the phenotypes may result from either specific or non-specific effects. If the effects are specific, these results could support an important role of *vgll3* during embryonic development in zebrafish, keeping in mind that the expression of the gene was ubiquitous during the earlier studied stages and the gene's knockdown seems to affect the whole embryo. However, with the use of morpholinos it is always good to be careful with interpretations of the results, because MOs may sometimes cause off-target and toxic effects even in relatively small doses. As it has been pointed out in a case of reduced Cytochrome C oxidase activity, MO injections can affect many cellular mechanisms (Baden *et al.* 2007). Even 1.0 ng of MO contains 2 x 10^{-4}-fold molar excess of antisense molecules compared to the abundance of an average mRNA molecule, which could potentially disturb the normal functions of a cell (Schulte-Merker & Stainier 2014). With the co-injections of p53 MO, I aimed to reduce the potential toxic effects of MO, but there is still a possibility that the injection could have activated another lethal pathway in the embryo. The morphants of all groups, except MO-group1, had typical malformations associated with toxicity such as necrosis in the head region, pericardial edema, and yolk sack edema (Bedell *et al.* 2011). Therefore, in addition to negative control MO and RNA rescue controls used in this work, other reliable validation methods such as groups injected with translation-blocking MO, MO targeting other splice site of the gene

or knockout mutants should be used (Eisen & Smith 2008; Nasevicius & Ekker 2000). For confirmation of the efficiency of MO, especially in the group without visible malformations, it is recommended to perform Western blotting or similar immunohistochemical technique. Other techniques such as qRT-PCR in order to detect the levels of mRNA molecules are also suitable (Eisen & Smith 2008).

In the overexpression experiment both injected groups showed malformations. The results of this experiment could support the results I documented in the knockdown experiment: both down- and upregulation of the expression of *vgll3* lead to developmental abnormalities. Potentially, even slight over-dosage of the *vgll3* product could have serious effects on early embryos. As with the knock-down experiment, it is also possible that occurred malformations are due to the toxicity of the injections. High concentrations of synthetic mRNA with combination of an early timing of injections could possibly result in dramatic phenotypes. In this experiment, I expected to see similar dose-dependent phenotypes as in the knockdown experiment, but surprisingly I observed more severe phenotypical changes in mRNA-group 1 receiving the lower dose and *vice versa*. One possible reason could be a technical error in mRNA dosage into the injection mixture, so the mixture with supposed higher mRNA concentration actually contained a lower concentration. Other possible reasons might be the quality of the spawning pairs and the offspring.

Frequencies of the hatched embryos in both injected groups were high despite of the high concentrations of mRNA in both groups, suggesting that fish injected with mRNA, although heavily mutated, were clearly more viable compared to the MO-injected fish. The result seemingly suggests that MO injections affect viability more than mRNA injections.

The mRNA rescue experiment to validate MO specificity was performed with coinjections of MO and mRNA. In cases of ubiquitous gene expression, the rescue method is usually straightforward (Eisen & Smith 2008). Unfortunately, the experiment did not produce expected results, and thus I could not validate MO phenotype from the knockdown experiment. The embryos from both injected groups showed some degree of malformations instead of expected rescued

WT-like phenotype. Both groups showed mixed mRNA overexpression and MO phenotypes with severe malformations. I documented higher degree of malformations in R-G2, what explains the low hatching rate in this group. I suggest that the combination of splice-blocking MO and mRNA was too toxic for early embryos. The most likely reason for toxicity is that I failed to achieve balanced dosage of both MO and mRNA resulting in either too high MO or mRNA dose, or both. Potentially, the results from all the experiments presented in this thesis might also be interpreted such that altering *vgll3* expression in any manner during the embryogenesis is harmful for the developing organism.

7 Conclusions

This thesis focused on characterizing the function of *VGLL3* that has been associated with variation in maturational timing in humans and Atlantic salmon, suggesting evolutionary conserved function of the gene. Since the main structures essential for puberty and sexual maturation, including the HPG-axis, start to develop during the embryogenesis, we hypothesized that *VGLL3* might contribute to the formation of these structures. To test this hypothesis, we examined the expression patterns and consequences of altering the expression levels of the *VGLL3* homolog in zebrafish embryos.

The findings from the experiments support the hypothesis of conserved functions of *VGLL3* among vertebrates, although we failed to link the gene with the development of the HPG axis. The ubiquitous nature of *vgll3* expression suggests that the gene contributes to the growth of zebrafish during the early stages of embryonic development. As the development proceeds, the expression localizes in the hindbrain and the midbrain-hindbrain boundary, suggesting *vgll3* may affect the formation of these structures. Manipulating *vgll3* expression resulted in malformed phenotypes, higher mortality and reduced hatching rate. Although the results from the experiments involving *vgll3* expression manipulation leave room for speculation, they do not completely exclude a potentially important role for *vgll3* during embryonic development.

8 Future directions

At the moment, we have continued the characterization of the *vgll3* by developing a knockout model for the *vgll3* gene with CRISPR/Cas9 system (Irion *et al.* 2014). We aim to study the impacts of a permanent gene knockout for fish vitality and development.

In this thesis, I was not able to study a possible role of *vgll3* for adipose tissue formation and accumulation, a potential function of *vgll3* known to affect maturational timing. Therefore, one interesting topic for the future could be evaluation of expression patterns and the effects of *vgll3* down- and upregulation in post 8 days old zebrafish. After this age, the development of fat cells occurs, and the study could yield links between *vgll3* and adipocyte formation (Flynn *et al.* 2009).

Another direction could be the evaluation of the role of *vgll3* for somitogenesis. According to the results presented in this thesis, the expression of *vgll3* is strong during the formation of the somites, and might play a role in this process.

9 Acknowledgements

I want to thank my supervisor Elisabeth Widén for letting me work in her group at FIMM and thus making this all possible. I also want to thank my second supervisor and mentor Jaakko Leinonen for all his enormous help. I am very grateful to director of Zebrafish Unit Pertti Panula for kindly allowing me to perform my experiments with fish in his unit. Zebrafish lab technicians Henri Koivula and Riikka Pesonen provided a huge help with handling zebrafish eggs, thank you! My family's support was also huge! The warm and friendly working environment made my hard and sometimes anxious working time much easier, thank you all for that!

References

Abraham, E. Palevitch, O. Gothilf, Y. & Zohar, Y. (2009). The zebrafish as a model system for forebrain GnRH neuronal development. *General and Comparative Endocrinology*, 164, 151-160.

Aksglaede, L. Olsen, L. W. Sorensen, T. I. & Juul, A. (2008). Forty years trends in timing of pubertal growth spurt in 157,000 Danish school children. *PLoS One*, 3, e2728.

Anderson, C. A. Zhu, G. Falchi, M. van den Berg, S. M. Treloar, S. A. Spector, T. D. … Montgomery, G. W. (2008). A Genome-Wide linkage scan for age at menarche in three populations of European descent. *The Journal of Clinical Endocrinology and Metabolism*, *93*, 3965–3970.

Ayllon, F. Kjærner-Semb, E. Furmanek, T. Wennevik, V. Solberg, M. F. Dahle, G. . . . Wargelius, A. (2015). The *vgll3* locus controls age at maturity in wild and domesticated Atlantic salmon (*Salmo salar* L.) Males. *PLoS Genet, 11*, e1005628.

Baden, K. N. Murray, J. Capaldi, R. A. and Guillemin, K. (2007). Early developmental pathology due to cytochrome C oxidase deficiency is revealed by a new zebrafish model. *J. Biol. Chem*. 282, 34839-34849.

Barbaux, S. Gascoin-Lachambre, G. Buffat, C. Monnier, P. Mondon, F. Tonanny, M.-B. . . . Vaiman, D. (2012). A genome-wide approach reveals novel imprinted genes expressed in the human placenta. *Epigenetics, 7*, 1079-1090.

Barson, N. J. Aykanat, T. Hindar, K. Baranski, M. Bolstad, G. H. Fiske, P. . . . Primmer, C. R. (2015). Sex-dependent dominance at a single locus maintains variation in age at maturity in salmon. *Nature, 528*, 405-408.

Bedell, V. M. Westcot, S. E. & Ekker, S. C. (2011). Lessons from morpholino-based screening in zebrafish. *Briefings in Functional Genomics*.

Bernard, F. Lalouette, A. Gullaud, M. Jeantet, A. Y. Cossard, R. Zider, A, Ferveur, F. J. & Silber, J. (2003). Control of apterous by vestigial drives indirect flight muscle development in drosophila. *Developmental Biology, 260*, 391-403.

Bill, B. R. Petzold, A. M. Clark, K. J. Schimmenti, L. A. & Ekker, S. C. (2009). A primer for morpholino use in zebrafish. *Zebrafish*, *6*, 69–77.

Blum, M. De Robertis, Edward M. Wallingford, John B. & Niehrs, C. (2015). Morpholinos: antisense and sensibility. *Developmental Cell, 35*, 145-149.

Cantor, R. M. Lange, K. & Sinsheimer, J. S. (2010). Prioritizing GWAS Results: A review of statistical methods and recommendations for their application. *American Journal of Human Genetics*, *86*, 6–22.

Chen, H.-H. Mullett, S. J. & Stewart, A. F. R. (2004a). Vgl-4, a novel member of the vestigial-like family of transcription cofactors, regulates α1-adrenergic activation of gene expression in cardiac myocytes. *Journal of Biological Chemistry, 279*, 30800-30806.

Chen, H.-H. Maeda, T. Mullett, S. J. & Stewart, A. F. R. (2004b). Transcription cofactor Vgl-2 is required for skeletal muscle differentiation. *genesis*, 39, 273-279.

Chen, W. & Ge, W. (2013). Gonad differentiation and puberty onset in the zebrafish: Evidence for the dependence of puberty onset on body growth but not age in females. *Mol Reprod Dev, 80*, 384-392.

Cheng, R. Ford, B. L. O'Neal, P. E. Mathews, C. Z. Bradford, C. S. Thongtan, T. . . . Bailey, G. S. (1997). Zebrafish (Danio rerio) p53 tumor suppressor gene: cDNA sequence and expression during embryogenesis. *Mol Mar Biol Biotechnol, 6*, 88-97.

Chevrier, L. Guimiot, F. & de Roux, N. (2011). GnRH receptor mutations in isolated gonadotropic deficiency. *Molecular and Cellular Endocrinology, 346*, 21-28.

Corey, D. R. & Abrams, J. M. (2001). Morpholino antisense oligonucleotides: tools for investigating vertebrate development. *Genome Biology*, *2*, reviews1015.1–reviews1015.3.

Cousminer, D. L. Berry, D. J. Timpson, N. J. Ang, W. Thiering, E. Byrne, E. . . . Consortium, f. t. E. G. G. (2013). Genome-wide association and longitudinal analyses reveal genetic loci linking pubertal height growth, pubertal timing, and childhood adiposity. *Human Molecular Genetics*, 22, 2735-2747.

Dooley, K. & Zon, L. I. (2000). Zebrafish: a model system for the study of human disease. *Current Opinion in Genetics & Development, 10*, 252-256.

Dubois, E. A. Zandbergen, M. A. Peute, J. & Goos Th, H. J. (2002). Evolutionary development of three gonadotropin-releasing hormone (GnRH) systems in vertebrates. *Brain Research Bulletin, 57*, 413-418.

Eisen, J. S. & Smith, J. C. (2008). Controlling morpholino experiments: don't stop making antisense. *Development, 135*, 1735-1743.

Elks, C. E. Perry, J. R. B. Sulem, P. Chasman, D. I. Franceschini, N. He, C. . . . Murray, A. (2010). Thirty new loci for age at menarche identified by a meta-analysis of genome-wide association studies. *Nat Genet, 42*, 1077-1085.

Faucheux, C. Naye, F. Tréguer, K. Fédou, S. Thiébaud, P. & Thézé, N. (2010). Vestigial like gene family expression in Xenopus: common and divergent features with other vertebrates. *International Journal of Developmental Biology*, *54*, 1375.

Fernald, R. D. & White, R. B. (1999). Gonadotropin-releasing hormone genes: phylogeny, structure, and functions. *Front Neuroendocrinol, 20*, 224-240.

Flynn, E. J. Trent, C. M. & Rawls, J. F. (2009). Ontogeny and nutritional control of adipogenesis in zebrafish (*Danio rerio*). *Journal of Lipid Research*, *50*, 1641–1652.

Golub, M. S. Collman, G. W. Foster, P. Kimmel, C. A. Meyts, E.R.-D. Reiner, E. O. Sharpe, R. M. Skakkebaek, N. E. Toppari, J. (2008). Public Health Implications of altered puberty timing. *Pediatrics*, *121*, 218-230.

Gajdos, Z. K. Henderson, K. D. Hirschhorn J. N. & Palmert, M. R. (2010). Genetic determinants of pubertal timing in the general population. *Molecular and Cellular Endocrinology*, 324, 21-29.

Gambaro, K. Quinn, M. C. Wojnarowicz, P. M. Arcand, S. L. de Ladurantaye, M. Barres, V. Ripeau, J. S. Killary, A. M. Davis, E. C. Lavoie, J. Provencher, D. M. Mes-Masson, A. M. Chevrette, M. & Tonin, P. N. (2013). VGLL3 expression is associated with a tumor suppressor phenotype in epithelial ovarian cancer. *Mol Oncol*, 7, 513-530.

Halperin, D.S. Pan, C. Lusis, A.J. & Tontonoz, P. (2013). Vestigial-like 3 is an inhibitor of adipocyte differentiation. *The Journal of Lipid Research*, 54, 473-481.

Hayes, H. & Dutrillaux, B. (2000) In situ hybridisation techniques. Techniques in Animal Cytogenetics (ed. by P.Popescu, H.Hayes and B. Dutrillaux), 69–84 Springer Verlag, Berlin.

He, C. Kraft, P. Chen, C. Buring, J. E. Pare, G. Hankinson, S. E. . . . Chasman, D. I. (2009). Genome-wide association studies identify loci associated with age at menarche and age at natural menopause. *Nat Genet, 41*, 724-728.

Hiatt, R.A. Haslam, S.Z. Osuch, J. (2009). The breast cancer and the environment research centers: transdisciplinary research on the role of the environment in breast cancer etiology. *Environmental Health Perspectives*, 117, 1814-1822.

Howe, K. Clark, M. D. Torroja, C. F. Torrance, J. Berthelot, C. Muffato, M. . . . Stemple, D. L. (2013). The zebrafish reference genome sequence and its relationship to the human genome. *Nature, 496*, 498-503.

Irion, U. Krauss, J. & Nüsslein-Volhard, C. (2014). Precise and efficient genome editing in zebrafish using the CRISPR/Cas9 system. *Development, 141*, 4827-4830.

Jin, L. & Lloyd, R. V. (1997). In situ hybridization: Methods and applications. *Journal of Clinical Laboratory Analysis, 11*, 2-9.

Kardash, E. (2012). Current methods in zebrafish research. MATER METHODS 2012;2:109.

Kennedy, G. C. & Mitra, J. (1963). Body weight and food intake as initiating factors for puberty in the rat. *J Physiol, 166*, 408-418.

Kimmel, C. B. Ballard, W. W. Kimmel, S. R. Ullmann, B. & Schilling, T. F. (1995). Stages of embryonic development of the zebrafish. *Dev Dyn, 203*, 253-310.

Kuiri-Hänninen, T. Sankilampi, U. Dunkel, L. (2014). Activation of the hypothalamic-pituitary-gonadal axis in infancy: minipuberty. *Hormone Research in Pediatrics*, 82, 73–80.

Lakshman, R. Forouhi, N.G. Sharp, S.J. Luben, R. Bingham, S.A. Khaw, K.T. Wareham, N.J. & Ong, K.K. (2009). Early age at menarche associated with cardiovascular disease and mortality. *The Journal of Clinical Endocrinology & Metabolism*, 94, 4953–4960.

Loesch, D.Z. Hopper, J.L. Rogucka, E. & Huggins, R.M. (1995). Timing and genetic rapport between growth in skeletal maturity and height around puberty: similarities and differences between girls and boys. *American Journal of Human Genetics*, 56, 753-759.

Mann, C. J. Osborn, D. P. S. & Hughes, S. M. (2007). Vestigial-like-2b (VITO-1b) and Tead-3a (Tef-5a) expression in zebrafish skeletal muscle, brain and notochord. *Gene Expression Patterns*, *7*, 827–836.

McDowell, E. N. Kisielewski, A. E. Pike, J. W. Franco, H. L. Yao, H. H. C. & Johnson, K. J. (2012). A Transcriptome-Wide Screen for mRNAs Enriched in Fetal Leydig Cells: CRHR1 Agonism Stimulates Rat and Mouse Fetal Testis Steroidogenesis. *PLoS ONE, 7*(10), e47359.

Meitinger, T. Heye, B. Petit, C. Levilliers, J. Golla, A. Moraine, C. … Ballabio, A. (1990). Definitive localization of X-linked Kallman syndrome (hypogonadotropic hypogonadism and anosmia) to Xp22.3: close linkage to the hypervariable repeat sequence CRI-S232. *American Journal of Human Genetics*, *47*, 664–669.

Mielcarek, M. Piotrowska, I. Schneider, A. Gunther, S. & Braun, T. (2009). VITO-2, a new SID domain protein, is expressed in the myogenic lineage during early mouse embryonic development. *Gene Expr Patterns, 9*, 129-137.

Morcos, P. A. (2007). Achieving targeted and quantifiable alteration of mRNA splicing with Morpholino oligos. *Biochem Biophys Res Commun, 358*, 521-527.

Morris, D. H. Jones, M. E. Schoemaker, M. J. Ashworth, A. & Swerdlow, A. J. (2011). Familial concordance for age at menarche: analyses from the Breakthrough Generations Study. *Paediatric and Perinatal Epidemiology, 25*, 306-311.

Nasevicius, A. & Ekker, S. C. (2000). Effective targeted gene 'knockdown' in zebrafish. *Nat Genet, 26*, 216-220.

Nelson, L. R. & Bulun, S. E. (2001). Estrogen production and action. *J Am Acad Dermatol, 45*, 116-124.

Okubo, K. & Nagahama, Y. (2008). Structural and functional evolution of gonadotropin-releasing hormone in vertebrates. *Acta Physiologica, 193*, 3-15.

Okuthe, G. M. Hanrahan, S. & Fabian, B. C. (2014). Early gonad development in zebrafish (Danio rerio). *African Journal of Biotechnology* , 13, 3433-3442.

Perry, J. R. B. Day, F. Elks, C. E. Sulem, P. Thompson, D. J. Ferreira, T. . . . Ong, K. K. (2014). Parent-of-origin-specific allelic associations among 106 genomic loci for age at menarche. *Nature, 514*, 92-97.

Pulst, S. M. (1999). Genetic Linkage Analysis. *Arch Neurol.,* 56, 667-672.

Raivio, T. Falardeau, J. Dwyer, A. Quinton, R. Hayes, F. J. Hughes, V. A. . . . Pitteloud, N. (2007). Reversal of Idiopathic Hypogonadotropic Hypogonadism. *New England Journal of Medicine, 357*, 863-873.

Robu, M. E. Larson, J. D. Nasevicius, A. Beiraghi, S. Brenner, C. Farber, S. A. & Ekker, S. C. (2007). p53 activation by knockdown technologies. *PLoS Genet, 3*, e78.

Rugarli, E. I. (1999). Kallmann Syndrome and the Link between Olfactory and Reproductive Development. *American Journal of Human Genetics*, 65, 943–948.

Schilling, T. F. Prince, V. E. & Ingham, P. W. (2001). Plasticity in Zebrafish hox Expression in the Hindbrain and Cranial Neural Crest. *Developmental Biology*, 231, 201-16.

Schulte-Merker, S. & Stainier, D. Y. (2014). Out with the old, in with the new: reassessing morpholino knockdowns in light of genome editing technology. *Development, 141*, 3103-3104.

Silverthorn, D. U. (2013). *Human physiology: An integrated approach*. San Francisco: Pearson Education.

Sisk, C. L. & Foster, D. L. (2004). The neural basis of puberty and adolescence. *Nat Neurosci, 7*, 1040-1047.

Sower, S. A. Freamat, M. & Kavanaugh, S. I. (2009). The origins of the vertebrate hypothalamic–pituitary–gonadal (HPG) and hypothalamic–pituitary–thyroid (HPT) endocrine systems: New insights from lampreys. *General and Comparative Endocrinology, 161*, 20-29.

Summerton, J. (1999). Morpholino antisense oligomers: the case for an RNase H-independent structural type. *Biochim Biophys Acta, 1489*, 141-158.

Sykiotis, G. P. Plummer, L. Hughes, V. A. Au, M. Durrani, S. Nayak-Young, S. . . . Pitteloud, N. (2010). Oligogenic basis of isolated gonadotropin-releasing hormone deficiency. *Proceedings of the National Academy of Sciences, 107*, 15140-15144.

Takezaki, N. Figueroa, F. Zaleska-Rutczynska, Z. & Klein, J. (2003). Molecular phylogeny of early vertebrates: monophyly of the agnathans as revealed by sequences of 35 genes. *Molecular Biology and Evolution, 20*, 287-292.

Tanner, J. M. Whitehouse, R. H. & Takaishi, M. (1966). Standards from birth to maturity for height, weight, height velocity, and weight velocity: British children, 1965. *Arch Dis Childh*, 41, 454-471. Retrieved from http://www.ncbi.nlm.nih.gov/pubmed/5957718

Taranger, G. L. Carrillo, M. Schulz, R. W. Fontaine, P. Zanuy, S. Felip, A. . . . Hansen, T. (2010). Control of puberty in farmed fish. *Gen Comp Endocrinol, 165*, 483-515.

Thisse, C. & Thisse, B. (2008). High-resolution in situ hybridization to whole-mount zebrafish embryos. *Nat. Protocols, 3*, 59-69.

Thisse, C. & Thisse, B. (2010). Thisse Lab - In Situ Hybridization Protocol – 2010 Update.

Thorpe, J. E. (2004). Life history responses of fishes to culture. *Journal of Fish Biology, 65*, 263-285.

Towne, B. Czerwinski, S. A. Demerath, E. W. Blangero, J. Roche, A. F. & Siervogel, R. M. (2005). Heritability of age at menarche in girls from the Fels Longitudinal Study. *Am J Phys Anthropol, 128*, 210-219.

Tu, W. Wagner, E. K. Eckert, G. J. Yu, Z. Hannon, T. Pratt, H. & He, C. (2014). Associations between menarche-related genetic variants and pubertal growth in male and female adolescents. *Journal of Adolescent Health*, 56, 66-72.

Vadakkadath Meethal, S. & Atwood, C. S. (2005). Alzheimer's disease: the impact of age-related changes in reproductive hormones. *Cellular and Molecular Life Sciences CMLS, 62*, 257-270.

Visscher, Peter M. Brown, Matthew A. McCarthy, Mark I. & Yang, J. (2012). Five Years of GWAS Discovery. *The American Journal of Human Genetics, 90*, 7-24.

Warren, L. Manos, P. D. Ahfeldt, T. Loh, Y.-H. Li, H. Lau, F. . . . Rossi, D. J. (2010). Highly Efficient Reprogramming to Pluripotency and Directed Differentiation of Human Cells with Synthetic Modified mRNA. *Cell Stem Cell, 7*, 618-630.

White, R. B. Eisen, J. A. Kasten, T. L. & Fernald, R. D. (1998). Second gene for gonadotropin-releasing hormone in humans. *Proc Natl Acad Sci U S A, 95*, 305-309.

Widén, E. Silventoinen, K. Sovio, U. Ripatti, S. Cousminer, D.L. Hartikainen, A.-L. Laitinen, J. Pouta, A. Kaprio, J. Järvelin, M.–R. Peltonen, L. Palotie, A. (2012). Pubertal timing and growth influences cardiometabolic risk factors in adult males and females. *Diabetes care*, 35, 850-856.

Wierman, M. E. Kiseljak-Vassiliades, K. & Tobet, S. (2011). Gonadotropin releasing hormone (GnRH) neuron migration: initiation, maintenance and cessation as critical steps to ensure normal reproductive function. *Frontiers in Neuroendocrinology*, 32, 43–52.

Xu, J. Huang, W. Zhong, C. Luo, D. Li, S. Zhu, Z. & Hu, W. (2011). Defining global gene expression changes of the hypothalamic-pituitary gonadal axis in female sGnRH-antisense transgenic common carp (*Cyprinus carpio*). *PLoS ONE*, *6*, e21057.

Yuan, S. & Sun, Z. (2009). Microinjection of mRNA and morpholino antisense oligonucleotides in zebrafish embryos. *Journal of Visualized Experiments : JoVE*, 27, 1113.

Appendices

ATTACHMENT 1.

ATTACHMENT 1. pGEM®-T Easy vector map (Promega)

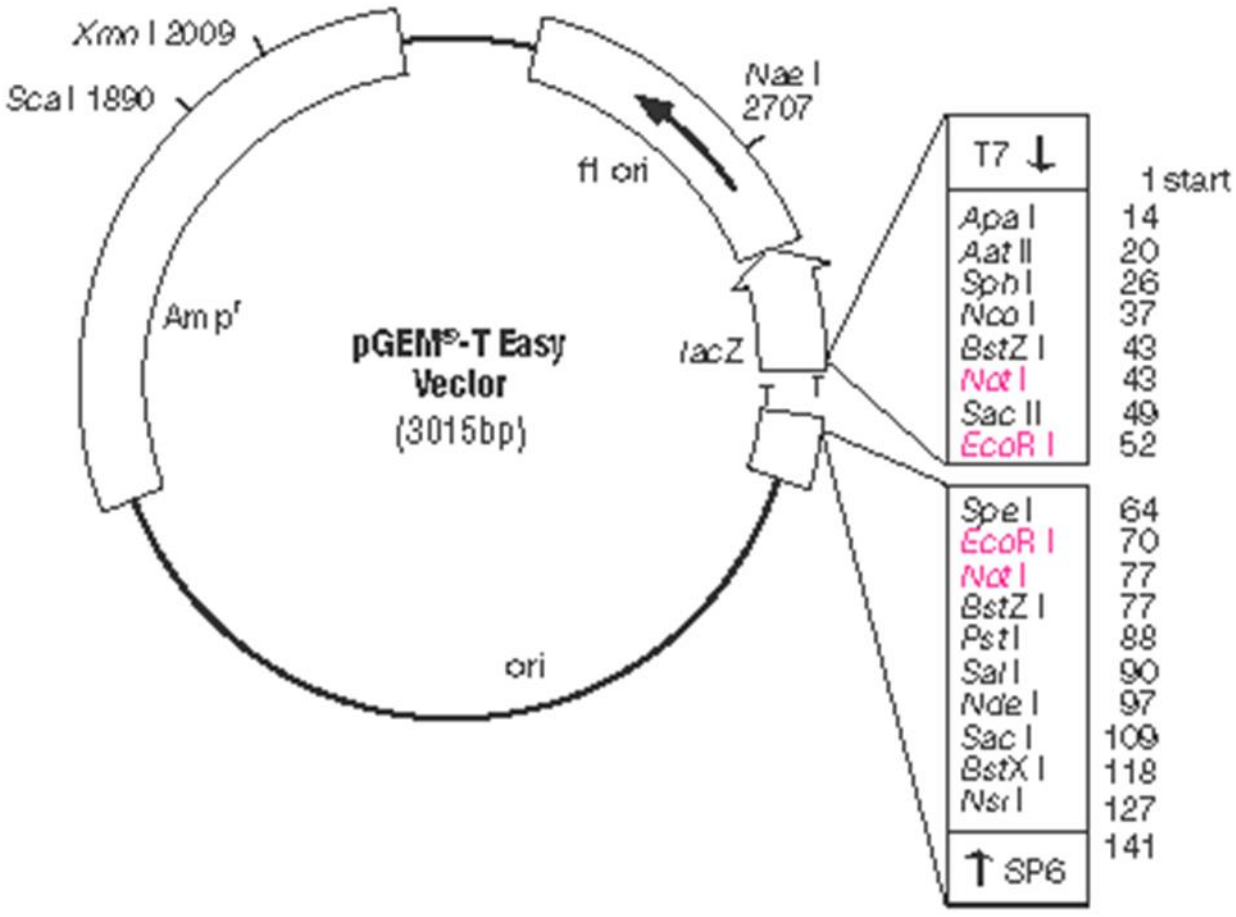

ATTACHMENT 2.

ATTACHMENT 2. A pMC plasmid used in the gene cloning